

RESEARCH ARTICLE

The osmorepiratory compromise: physiological responses and tolerance to hypoxia are affected by salinity acclimation in the euryhaline Atlantic killifish (*Fundulus heteroclitus*)

Marina Giacomini^{1,2,*}, Heather J. Bryant¹, Adalberto L. Val³, Patricia M. Schulte¹ and Chris M. Wood^{1,2,4}

ABSTRACT

The characteristics of the fish gill that maximize gas exchange are the same that promote diffusion of ions and water to and from the environment; therefore, physiological trade-offs are likely to occur. Here, we investigated how salinity acclimation affects whole-animal respiratory gas exchange during hypoxia using *Fundulus heteroclitus*, a fish that inhabits salt marshes where salinity and oxygen levels vary greatly. Salinity had marked effects on hypoxia tolerance, with fish acclimated to 11 and 35 ppt showing much longer time to loss of equilibrium (LOE) in hypoxia than 0 ppt-acclimated fish. Fish acclimated to 11 ppt (isosmotic salinity) exhibited the greatest capacity to regulate oxygen consumption rate (\dot{M}_{O_2}) under hypoxia, as measured through the regulation index (RI) and P_{crit} . At 35 ppt, fish had a higher routine metabolic rate (RMR) but a lower RI than fish at 11 ppt, but there were no differences in gill morphology, ventilation or blood O_2 transport properties between these groups. In contrast, 0 ppt-acclimated fish had the highest ventilation and lowest O_2 extraction efficiency in normoxia and hypoxia, indicating a higher ventilatory workload in order to maintain similar levels of \dot{M}_{O_2} . These differences were related to alterations in gill morphology, where 0 ppt-acclimated fish had the smallest lamellar surface area with the greatest epithelial cell coverage (i.e. thicker lamellae, longer diffusion distance) and a larger interlamellar cell mass, contrasting with 11 ppt-acclimated fish, which had overall the highest respiratory surface area. The alteration of an array of physiological parameters provides evidence for a compromise between salinity and hypoxia tolerance in killifish acclimated to freshwater.

KEY WORDS: Ion regulation, Metabolic rate, Trade-offs

INTRODUCTION

In recent years, the occurrence and severity of aquatic hypoxia have greatly increased as a result of a variety of anthropogenic factors, including pollution, eutrophication and climate change (Ficke et al., 2007; Díaz and Breitburg, 2011). The major threat posed by hypoxia is the potential mismatch between oxygen demand and supply within the organism. Fish facing hypoxia can employ mechanisms to either increase O_2 uptake from the water or reduce utilization by depression of metabolic demand (Hochachka et al., 1996). Branchial oxygen

uptake can be improved by increasing gill ventilation and perfusion (Perry et al., 2009). Fish can also enhance gill oxygen transfer through increases in the functional respiratory surface area of the gill by redirecting blood flow from marginal circulatory shunts to central channels within the lamellae (Nilsson et al., 1995; Sundin and Nilsson, 1998). Blood O_2 carrying capacity can also be modified through increases in haematocrit and haemoglobin content, and haemoglobin O_2 affinity can be modified through changes in the concentration of allosteric modifiers (Val, 2000). A more recently discussed strategy is the rapid reversible alteration of gill morphology (Nilsson, 2007), where fish quickly shed the interlamellar cell mass (ILCM) that fills the interlamellar channels (Sollid et al., 2003), thereby reducing the distance for diffusion between blood and water.

The gills are the primary site for both ion and respiratory gas exchange, so trade-offs between the optimal structures for these processes occur. This phenomenon has been called the osmorepiratory compromise (Randall et al., 1972; Gonzalez and McDonald, 1992), where the conflict between the need for high gill permeability for respiratory gas exchange and the need for low gill permeability to limit ion diffusion can cause physiological impairment (Gilmour and Perry, 2018). Movement between salinities that range from freshwater (FW) to seawater (SW) poses an osmoregulatory challenge for euryhaline fishes, one which may have respiratory consequences. This challenge involves the transformation of the gill epithelium from a salt-absorbing surface in FW to a salt-secreting surface in SW (Evans et al., 2005; Edwards and Marshall, 2013). In the euryhaline *Fundulus heteroclitus*, this transformation is characterized by remarkable changes in ion transporter density (Katoh and Kaneko, 2003), the morphology of the ion-transporting cells (ionocytes) and the distribution of these cells within the gill epithelia (Laurent et al., 2006). This modulation of gill morphology may result in increased barrier thickness in order to facilitate favourable active ion transport and limit unfavourable passive ion diffusion. However, these modifications might be detrimental to whole-animal respiratory capacity, as the blood-to-water diffusion distance for gas exchange also increases. This has been shown in several studies with FW fishes (Thomas et al., 1988; Greco et al., 1996; Perry, 1998; Sollid et al., 2003; Henriksson et al., 2008). For example, an investigation comparing two species of sculpin showed that the species with the higher FW tolerance had a greater diffusion distance and lower surface area, which resulted in a compromised tolerance to hypoxia (Henriksson et al., 2008).

Our goal was to investigate how salinity acclimation affects whole-animal respiratory gas exchange using an integrative approach on the Atlantic killifish *Fundulus heteroclitus* as a model. This species is native to estuaries and salt marshes from northeastern Florida, USA, to the Gulf of St Lawrence, Canada, occasionally entering FW environments (Taylor et al., 1979), and is well known for its remarkable euryhalinity, rapidly adjusting its

¹Department of Zoology, The University of British Columbia, Vancouver, BC, Canada V6T 1Z4. ²Bamfield Marine Sciences Centre, Bamfield, BC, Canada V0R 1B0. ³Laboratory of Ecophysiology and Molecular Evolution, Instituto Nacional de Pesquisas da Amazônia (INPA), Manaus, Amazonas 69080-971, Brazil. ⁴Department of Biology, McMaster University, Hamilton, ON, Canada L8S 4K1.

*Author for correspondence (giacomini@zoology.ubc.ca)

© M.G., 0000-0002-8163-3285; H.J.B., 0000-0002-8553-7792; A.L.V., 0000-0002-3823-3868; P.M.S., 0000-0002-5237-8836; C.M.W., 0000-0002-9542-2219

List of symbols and abbreviations

FW	freshwater
Hb	haemoglobin
Hct	haematocrit
ILCM	interlamellar cell mass
K_m	affinity constant
LOE	loss of equilibrium
MCHC	mean cell haemoglobin concentration
M–M	Michaelis–Menten
\dot{M}_{O_2}	rate of oxygen consumption
n_{50}	Hill coefficient
NTP	nucleoside triphosphate (organic phosphates ATP and GTP)
OEC	oxygen equilibrium curve
P_{50}	P_{O_2} at which Hb is 50% saturated with oxygen
P_{CO_2}	partial pressure of carbon dioxide
P_{crit}	critical oxygen tension
P_{O_2}	partial pressure of oxygen
RBC	red blood cell
RI	regulation index
RMR	routine metabolic rate
SA	surface area
SW	seawater
ϕ	Bohr coefficient

physiology when transferred from FW to greater than full-strength SW (Griffith, 1974). Killifish are also tolerant of hypoxia, for which they also serve as a model (Cochran and Burnett, 1996; Richards et al., 2008; McBryan et al., 2016). Despite their well-accepted status as model organisms in both fields (Burnett et al., 2007), there are few studies that have examined the interactive effects of respiratory gas exchange and ionoregulation under conditions of hypoxia and salinity variation. Blewett et al. (2013) found that the oxygen consumption rate (\dot{M}_{O_2}) was greater during hypoxia at intermediate salinity (16 ppt) than in killifish acclimated to FW or 100% SW. Wood and Grosell (2015) reported that hypoxia had quantitatively similar effects in depressing gill transepithelial potential in FW- and SW-acclimated killifish, though the mechanisms were probably different.

The salinity at which the internal osmotic pressure of the fish is the same as that of the water is known as the isosmotic point. Theory predicts that the energetic cost of osmoregulation should be lowest in an isosmotic environment (Boeuf and Payan, 2001), as the ionic gradients between blood and water would be minimal. Thus, the energy allocated for ionoregulation and osmoregulation should be negligible, allowing for more energy availability during low oxygen exposure. Additionally, as the need for active ionoregulation and osmoregulation is minimized, the performance of the respiratory system for O_2 uptake should be maximized. Because of the effects of the osmoregulatory compromise stated above, acclimation to other salinities could elicit gill morphology alterations with the potential to impair whole-animal respiratory capacity and, as a consequence, the ability to deal with hypoxia.

Thus, we predicted that acclimation to the isosmotic salinity (approximately 11 ppt for *F. heteroclitus*) would result in the greatest hypoxia tolerance, with lower tolerance in FW (0 ppt) and full-strength SW (35 ppt), and that isosmotic salinity would also result in the greatest capacity to regulate oxygen consumption under hypoxia. Furthermore, we predicted that salinity-related changes in gill morphology would reduce gill oxygen permeability in order to favour ionic homeostasis and active ion transport, and that this would have an effect on hypoxia tolerance. Additionally, we predicted that such differences would be reflected in the respiratory

and ventilatory responses of the fish to hypoxia, as well as their blood O_2 transport characteristics and gill morphology.

MATERIALS AND METHODS**Fish acclimation**

Fundulus heteroclitus macrolepidotus (Linnaeus 1766) (northern subspecies) were collected by Aquatic Research Organisms (Inc.) near Hampton, NH, USA (42°54'46''N) and shipped overnight to the University of British Columbia where they were held in groups of ~25 fish per 120 l tank at 18°C, under a photoperiod of 12 h light:12 h dark. Salinity was achieved by mixing Instant Ocean Aquarium Salt (Instant Ocean, Spectrum Brands, Blacksburg, VA, USA) with Vancouver dechlorinated tap water, and was monitored with a conductivity meter (Cond 3310, WTW, Xylem Analytics, Weilheim, Germany). Fish were fed daily to satiation with commercial fish flakes (Nutrafin Max Tropical Flakes, Mansfield, MA, USA). All fish were acclimated for a minimum of 4 weeks at each salinity and fasted for 24 h prior to all experimentation. Experiments were performed at the acclimation salinity, at 18–20°C. All experiments were conducted following the guidelines of the Canada Council for Animal Care, under approval of the animal care committee at the University of British Columbia (AUP A14-0251).

Time to loss of equilibrium in hypoxia

Separate groups of fish ($n=8-10$ per salinity; mean body mass 3.80 ± 0.22 g) were used for this experimental series, each acclimated to a different salinity (0, 3, 11, 15 and 35 ppt). Time to loss of equilibrium (LOE) in hypoxia was determined simultaneously for the five different salinities. Fish were placed in individual plastic chambers, where two of the sides had been replaced with a fine plastic mesh allowing the water to flow freely inside. The chambers were weighted down, so that the whole chamber was submerged, preventing killifish from performing aquatic surface respiration. A stick was fitted on the lid of each chamber, allowing chamber manipulation without disturbing the fish inside. Chambers were placed in 30 l Plexiglas tanks, one for each salinity. Each 30 l tank contained a small submersible recirculating water pump and an air stone. Fish were placed in the set-up overnight, prior to the beginning of the trial on the next day, at which time 50% of the water was replaced by gentle syphoning. Oxygen was reduced from normoxia (155 Torr; note 1 Torr=0.13332 kPa) to severe hypoxia (3.5 Torr) over approximately 1 h, and maintained at this level by bubbling the tanks with either compressed N_2 or air. Water partial pressure of oxygen (P_{O_2}) was monitored throughout the duration of the trials using the same hand-held oxygen meter (Accumet AP84A, Fisher Scientific, Toronto, ON, Canada), calibrated identically and checked repeatedly. Time to LOE was defined as the time (in hours) after the water reached 3.5 Torr until the fish lost equilibrium. LOE was determined as the point when a fish had settled at the bottom of the chamber, on its side or upright, and was no longer responding to a gentle movement of the chamber. After removal from the chambers, fish were weighed, and allowed to recover in a separate tank.

Oxygen consumption rate (\dot{M}_{O_2})

Separate groups of fish ($n=8$ per salinity; mean body mass 3.83 ± 0.12 g) were used for this experimental series. \dot{M}_{O_2} ($\mu\text{mol } O_2 \text{ g}^{-1} \text{ h}^{-1}$) under routine conditions was determined using closed-system respirometry, at 18°C, with water at the salinity to which the fish had been acclimated (0, 11 and 35 ppt). Each respirometer consisted of a rectangular 220 ml glass jar containing a small magnetic stir bar, physically separated from the fish by a piece of mesh, plus two ports, each one closed with a rubber stopper. The chambers were placed

inside a water bath to maintain a constant temperature of 18°C, over a stir-plate to ensure adequate mixing inside the chambers. Fish were placed in the respirometers overnight under flow-through conditions. At the beginning of the trial, a probe (FOXY-R, Ocean Optics Ltd, Largo, FL, USA) was inserted in each chamber, water flow was stopped, the chamber was sealed, and water P_{O_2} was monitored over time (sampling rate every 20 s), until P_{O_2} reached ~ 0 Torr. The chambers were rinsed daily with ethanol to eliminate any bacterial build-up. A blank (respirometer with no fish) trial was performed for every four fish, and oxygen consumption was negligible. On average, trials lasted 175 ± 13 min. The average fish mass to respirometer volume ratio was 0.015 ± 0.0005 g ml⁻¹. The slope of decreasing water P_{O_2} versus time was computed every 5 min, and \dot{M}_{O_2} ($\mu\text{mol g}^{-1} \text{h}^{-1}$) was calculated by:

$$\dot{M}_{O_2} = (\Delta P_{O_2} \times \alpha_{O_2} \times V) / M, \quad (1)$$

where ΔP_{O_2} is the slope of P_{O_2} over time (h), α_{O_2} is the solubility constant ($\mu\text{mol O}_2 \text{Torr}^{-1} \text{l}^{-1}$) in water at 18°C and at the appropriate salinity (Boutilier et al., 1984), M is body mass (g) and V is the respirometer volume (l). Data were binned at 5 Torr intervals.

The regulation index (RI) as described by Mueller and Seymour (2011), and originally conceived by Alexander and McMahon (2004), was calculated for the three salinities individually on an individual fish basis, using procedures recommended by Wood (2018). Briefly, \dot{M}_{O_2} versus P_{O_2} plots were fitted with a Michaelis–Menten (M–M) curve:

$$\dot{M}_{O_2} = (\text{Routine } O_{2,\text{max}} \times P_{O_2}) / (K_m + P_{O_2}), \quad (2)$$

where, by analogy to enzyme kinetics, \dot{M}_{O_2} is the rate, P_{O_2} is the substrate concentration, and the equation allows us to obtain routine $O_{2,\text{max}}$ and the affinity constant (K_m) of the organism for oxygen. The M–M curve yielded the highest r^2 when compared with other curve fits in Graph Pad Prism (v.5; Graph Pad Software, San Diego, CA, USA), including a sigmoidal modification based on the Hill equation as another possibility suggested by Wood (2018). This M–M curve was then compared with a linear regression constructed using the \dot{M}_{O_2} value at the start of the curve (P_{O_2} of air saturation) and at the end of the curve (the P_{O_2} where \dot{M}_{O_2} became 0). Both the M–M curve and the straight line were integrated and the area under the curve between the two lines was calculated. Additionally, a straight horizontal line was plotted starting at the \dot{M}_{O_2} at the highest P_{O_2} , representing a hypothetical situation where the fish regulates \dot{M}_{O_2} at all P_{O_2} levels. The area under the M–M curve was expressed as a proportion of the 100% regulation area, so a RI value of 1 would indicate perfect regulation, while a value of 0 would indicate a perfect conformation. Therefore, the RI is used as an indication of the regulatory ability of the fish.

The critical oxygen tension (P_{crit}) is another indicator of the regulatory ability of the fish. P_{crit} is defined as the transition P_{O_2} where \dot{M}_{O_2} is no longer independent of environmental P_{O_2} and becomes dependent. In other words, P_{crit} is the inflexion point where a fish is no longer an oxyregulator and becomes an oxyconformer (Pörtner and Grieshaber, 1993). P_{crit} was determined using the greatest difference method (Mueller and Seymour, 2011), where the P_{O_2} at which the vertical distance between the M–M curve and the straight line describing 100% conformity was the greatest. Routine metabolic rate (RMR) under non-limiting conditions was calculated as the average \dot{M}_{O_2} at the start of the trial, where P_{O_2} was highest (>90 Torr).

Ventilation during progressive hypoxia

Separate groups of fish ($n=11$ – 12 per salinity; mean body mass 5.58 ± 0.22 g) were used for this experimental series. Killifish were anaesthetized with 0.5 g l^{-1} MS-222 (Syndel Laboratories, Nanaimo, BC, Canada) buffered with HCO_3^- and fitted with a buccal catheter for the recording of ventilatory pressure and amplitude. A short length of plastic tubing (~ 2 cm, PE160 BD, Intramedic, Franklin Lakes, NJ, USA), flared on the buccal side, was inserted snugly into a hole made in the rostrum using a 19-gauge hypodermic needle. A slightly longer piece of PE50 tubing, also flared, was threaded through the PE160 sleeve, and the two pieces were glued together with a drop of cyanoacrylate glue, and then secured in place with a silk suture on the outer side of the hole. Fish were allowed to recover from the procedure overnight, in the same individual plastic chambers as used in the LOE experiments (see ‘Time to loss of equilibrium in hypoxia’, above). The chambers were placed in a darkened bath filled with water of the salinity to which the fish had been acclimated (0, 11 and 35 ppt).

For the measurements of ventilation, the water-filled internal PE50 catheter was bridged to a longer (50 cm) piece of tubing using the shaft of a 22-gauge blunted needle, and then connected to a pressure transducer (DPT-100, Utah Medical Products, Midvale, UT, USA) so that the ventilatory pressure amplitude (cmH₂O) and frequency (breaths min⁻¹) could be recorded. The pressure transducer was calibrated daily to a 4 cm water column. Water P_{O_2} was gradually lowered at a rate of ~ 1.15 Torr min⁻¹ using compressed N₂ gas, bubbled into a reservoir from which water flowed to the water bath, so as to avoid any external source of stimuli and to decrease stress. P_{O_2} was lowered from ~ 150 Torr to ~ 2 Torr over a period of about 130 min, a rate similar to that in the \dot{M}_{O_2} series [see ‘Oxygen consumption rate (\dot{M}_{O_2})’, above], and ventilation was constantly recorded using a PowerLab Data Integrity system (ADInstruments, Colorado Springs, CO, USA), connected to an amplifier (LCA-RTC, Transducer Techniques, Temecula, CA, USA), and visualized and analysed using LabChart v.7.0 (ADInstruments). Recordings of ventilation frequency (breaths min⁻¹) and pressure amplitude (cmH₂O breath⁻¹) were averaged every 5 min, and plotted against the average P_{O_2} at each time interval. The ventilatory index (cmH₂O min⁻¹) was calculated as follows:

$$\text{Ventilatory index} = \text{frequency} \times \text{pressure amplitude}, \quad (3)$$

where frequency is in breaths min⁻¹ and amplitude is in cmH₂O. Data were binned at 5 Torr intervals. Water P_{O_2} was monitored throughout the duration of the trials using a hand-held oxygen meter (Accumet AP84A, Fisher Scientific). All progressive hypoxia exposures were performed at the salinity of acclimation.

Hypoxia exposure for blood and tissue sampling

Separate groups of fish ($n=6$ – 8 per salinity; mean body mass 4.05 ± 0.18 g) were used for this experimental series. The same experimental chambers and apparatus described above (‘Time to loss of equilibrium in hypoxia’) were used for the two experiments in this series. Fish were placed in the chambers and allowed to settle overnight; 50% of the water was replaced prior to the start of the trial. P_{O_2} was reduced from normoxia (155 Torr) to hypoxia (15 Torr) over 1 h and maintained at this level with compressed N₂ and air. Killifish were kept in hypoxia for 3 h, and then immediately anaesthetized in 0.5 g l^{-1} buffered MS-222, and blood samples were quickly drawn by caudal puncture using a modified gas-tight Hamilton (100 μl) syringe (Reno, NV, USA). Normoxic fish underwent the same protocol, but P_{O_2} was kept in normoxia. All fish

used for the analysis of blood parameters and gill morphometrics underwent this regime. After blood sampling, the anaesthetized fish were killed by severing the spinal cord.

Whole-blood oxygen affinity (P_{50})

Once withdrawn, blood samples were kept on ice until analysis, and then transferred to a micro-tonometer at the experimental temperature, fashioned after the one described in Wood et al. (2010). Blood pH (~40 to 50 μ l) was measured twice, after two different equilibration steps, where samples were equilibrated for 30 min to physiological partial pressure of carbon dioxide (P_{CO_2}) (1.9 Torr; P_{O_2} =155 Torr) and to a high P_{CO_2} (7.6 Torr; P_{O_2} =155 Torr). Gas mixtures were obtained using DIGAMIX gas mixing pumps (H. Wösthoff Messtechnik, Bochum, Germany), and blood pH was measured using an oesophageal micro-pH electrode (MI-508; Microelectrodes Inc., Bedford, NH, USA).

Oxygen equilibrium curves (OEC) were generated using the spectrophotometric technique described by Lilly et al. (2013), adapted for a 96-well microplate spectrophotometer (SpectraMax 190; Molecular Devices, Sunnyvale, CA, USA). Fresh whole blood (1.8 μ l) was sandwiched between two thin layers of gas-permeable low-density polyethylene, secured on a small aluminium ring by two plastic O-rings and placed in a gas-tight tonometry cell modified to fit into the microplate reader. Hb O_2 saturation was determined spectrophotometrically at nine different P_{O_2} values obtained by mixing compressed O_2 and N_2 in various ratios using the Wösthoff pumps, starting from 0 Torr (fully deoxygenated), working towards 155 Torr (fully oxygenated). All spectrophotometric analyses were done at 18°C and at two separate P_{CO_2} levels (1.9 and 7.6 Torr). A logistic model designed to fit blood samples with multiple haemoglobin isoforms was fitted through the percentage blood O_2 saturation versus P_{O_2} data for each fish in order to determine blood P_{O_2} at which Hb is 50% saturated with oxygen (P_{50}) in R (v.3.1.2; Public domain):

$$y = d / (1 + \exp[\log_{10}(x/e)^b]), \quad (4)$$

where y is the fractional O_2 saturation, x is the P_{O_2} at each equilibration step, and d , b and e are the equation parameters: d is the upper asymptote of the model, b is Hill's slope and e is the inflexion point. After the determination of P_{50} , Eqn 4 was derived and the Hill coefficient at P_{50} (n_{50}) was obtained:

$$n_{50} = -b(\exp[b(\log_{10}P_{50})]) / [-1(-1 + d)(e^{(b/\ln 10)}) + \exp[b(\log_{10}P_{50})](\ln 10)]. \quad (5)$$

The Bohr coefficient (Φ) was calculated as follows:

$$\Phi = [\log_{10}P_{50(1.9 \text{ Torr})} - \log_{10}P_{50(7.6 \text{ Torr})}] / [\text{blood pH}_{(1.9 \text{ Torr})} - \text{blood pH}_{(7.6 \text{ Torr})}], \quad (6)$$

where $\log_{10}P_{50(1.9 \text{ Torr})}$ is the logarithm of whole-blood P_{50} assayed at P_{CO_2} of 1.9 Torr, $\log_{10}P_{50(7.6 \text{ Torr})}$ is the logarithm of whole-blood P_{50} assayed at P_{CO_2} of 7.6 Torr, $\text{blood pH}_{(1.9 \text{ Torr})}$ is the blood pH after equilibration at 1.9 Torr P_{CO_2} and $\text{blood pH}_{(7.6 \text{ Torr})}$ is the blood pH after equilibration at 7.6 Torr P_{CO_2} .

Haematocrit, haemoglobin concentration and red blood cell NTP extraction and analysis

Haematocrit (Hct) was measured as the percentage of packed RBCs (% RBC) within the total blood volume after centrifugation in micro-haematocrit tubes (2 \times 5 μ l) for 10 min at 10,000 g . Whole-blood haemoglobin concentration ([Hb]: mmol l⁻¹ blood) was measured

spectrophotometrically at 540 nm using Drabkin's reagent (Sigma-Aldrich, St Louis, MO, USA), with a spectrophotometer (Shimadzu UV-160, Kyoto, Japan), and calculated with a millimolar extinction coefficient of 11 (Völkel and Berenbrink, 2000). Mean cell haemoglobin concentration (MCHC: mmol Hb l⁻¹ RBC) was calculated as follows:

$$\text{MCHC} = [\text{Hb}] / (\text{Hct}/100). \quad (7)$$

RBC nucleoside triphosphates (NTPs; ATP and GTP) were extracted from freshly drawn blood according to the protocol described in Bartlett (1978). Briefly, immediately after sampling, blood samples were acidified with 0.6 mol l⁻¹ perchloric acid, centrifuged, and the supernatant neutralized with 6 mol l⁻¹ KOH. The precipitate was discarded, and the extracts were kept frozen (-80°C) until chromatographic analysis. For the analysis, samples were thawed and centrifuged three times (5 min at 14,000 rpm) for maximum elimination of salts and protein debris. A 10 μ l sample was collected and diluted in 990 μ l of 2 mmol l⁻¹ aqueous ammonium acetate solution. The analysis was performed using high-performance liquid chromatography coupled to mass spectrometry (LC-MS/MS; ESI 4000, Qtrap, ABSCIEX, Concord, ON, Canada) in MRM mode by monitoring the characteristic mass/charge ratio (m/z) transitions for ATP (506.0>158.8) and GTP (522.2>158.8). The runs were conducted in mobile phase of 2 mmol l⁻¹ ammonium acetate, with a flow rate of 125 μ l min⁻¹, using a Zorbax Eclipse XBD-C18 chromatographic column for 6 min. A standard curve was made with eight points from serial dilutions (0.5–50 μ mol ml⁻¹) of a solution containing ATP and GTP (ATP R^2 =0.9989; GTP R^2 =0.9991). Standards were measured every five samples. Measurements were performed in triplicate.

Gill morphometrics and morphology

Fish used for this experimental series underwent the same protocol as described above in 'Hypoxia exposure for blood and tissue sampling' but were kept in normoxia throughout the duration of the experiment. Once fish had lost equilibrium in anaesthetic (0.5 g l⁻¹ buffered MS-222), they were weighed, the spinal cord severed and the entire gill basket carefully excised. The gills were fixed in 2 ml Karnovsky's fixative (25% glutaraldehyde, 16% formaldehyde, 0.16 mol l⁻¹ sodium phosphate buffer, pH 7.2) for 24 h at 4°C. Samples were then transferred to 0.1 mol l⁻¹ sodium cacodylate buffer (pH 7.2) and stored at 4°C until use. The second gill arch was isolated from the gill basket and its anterior hemibranch imaged using a light microscope (SZX10 stereomicroscope; Olympus, Tokyo, Japan) at 4–6.3 \times magnification, and images were captured using cellSens software (v.1.12; Olympus), digitized and measured using ImageJ v.1.50i (Public domain). Care was taken to ensure that all images were taken at a consistent orientation that provided unbiased measurements. Total gill surface area was estimated according to Wegner (2011). After the total number of filaments had been counted on the intact hemibranch, the length of the gill arch was divided into five sections, and further measurements were made on the isolated central filament of each of the five sections. Each filament was imaged from two different orientations (top and side), allowing clear views of its own length, additionally to the height (distance from base to the distal edge of the lamellae), length and width of the lamellae. More specifically, these were measured on three lamellae per filament (one located at the base, one from the middle and one from the tip), as well as the width of the water channels located in between two lamellae. Each

filament's lamellar frequency (number lamellae μm^{-1} , F_{lamellae}) was estimated as:

$$F_{\text{lamellae}} = L_{\text{filament}} / (W_{\text{lamella}} + W_{\text{channel}}), \quad (8)$$

where L_{filament} is the total filament length (μm), W_{lamella} is the average lamellar width (μm) and W_{channel} is the average channel width (μm). Individual lamellar surface area for each of the three lamellae measured was estimated as the product of lamellar height and lamellar basal length. The total surface area of the lamellae on each filament (SA_{FL} : μm^2) was obtained from the mean individual lamellar surface area multiplied by the total number of lamellae per filament multiplied by 4, so as to account for the two faces of each lamella and the lamellae present on both sides of the filament. Finally, the mass-specific second gill arch lamellar surface area (SA_{total} : $\mu\text{m}^2 \text{g}^{-1}$) for both sides of the gill basket for each fish was calculated as:

$$\text{SA}_{\text{total}} = (\text{SA}_{\text{FL}} \times N_{\text{filaments}} \times 4) / M, \quad (9)$$

where SA_{FL} is the mean lamellar surface area of the five analysed filaments, $N_{\text{filaments}}$ is the number of filaments per gill arch, multiplication by 4 accounts for the two sides of the hemibranch multiplied by the two sides of the gill basket, and M is the body mass (g).

For the histological analyses, the entire third gill arch was embedded in paraffin wax and serologically sectioned at 5 μm thickness, mounted and stained with Hematoxylin and Eosin at Wax-it Histology Services Inc. (University of British Columbia). Eighteen sections per fish were divided between four slides containing 4–5 sections each and imaged using an inverted microscope (AE31; Motic, Hong Kong, China) at 400 \times magnification. ILCM (μm^2), epithelial cell layer area (μm^2) and ionocyte density at the filament (number of cells μm^{-2}) for randomly selected sections were measured using ImageJ v.1.52a while the observer was blind to treatment groups. For each fish, 40–60 ILCM measurements (15 per slide), 30–32 epithelial cell layer area measurements (8–17 per slide) and 8–10 ionocyte density measurements (2–5 per slide) were taken. A diagram detailing the measurements is shown in the Results. ILCMs, lamellae and gill areas were randomly selected within each image for the respective measurements. Epithelial cell layer coverage was expressed per unit height of the lamellae ($\mu\text{m}^2 \mu\text{m}^{-1}$).

Statistical analyses

All data are shown as means \pm 1 s.e.m. (n =number of animals). Detailed results of the statistical tests and *post hoc* analyses are shown in specific figure captions. ANOVA assumptions (data normality and homogeneity of variances) were checked, and if not achieved, data were transformed using a log transformation. For the one-way ANOVA, mean values were considered significantly different when $P < 0.05$. For the two-way ANOVA *post hoc* tests, the Bonferroni correction for multiple comparisons was applied.

RESULTS

Time to LOE in hypoxia

Salinity acclimation had a significant effect on time to LOE in hypoxia in killifish ($P < 0.001$; Fig. 1). Fish acclimated to a salinity of 0 ppt maintained their normal dorso-ventral orientation for 2.2 h and then lost equilibrium, while fish acclimated to 11 ppt (isosmotic point) maintained equilibrium for the longest time (~ 18 h), which did not differ significantly from that of fish acclimated to 35 ppt (Fig. 1). Fish acclimated to 3 and 15 ppt exhibited intermediate tolerance.

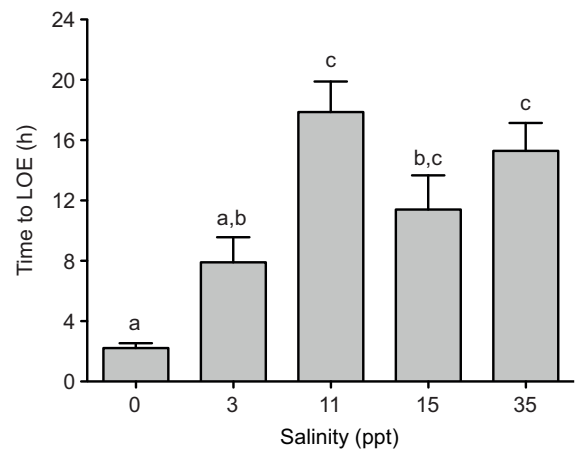


Fig. 1. Time to loss of equilibrium (LOE) in hypoxia (3.5 Torr) in *Fundulus heteroclitus* acclimated to a salinity of 0, 3, 11, 15 and 35 ppt. Data are means \pm s.e.m. ($n=8$). Bars sharing the same lowercase letters are not statistically different (one-way ANOVA).

Oxygen consumption rate (\dot{M}_{O_2})

Fig. 2A–C shows the \dot{M}_{O_2} versus P_{O_2} relationships of killifish acclimated to 0, 11 and 35 ppt. While fish at 0 and 11 ppt exhibited similar \dot{M}_{O_2} responses with decreasing P_{O_2} , the pattern seen for 35 ppt-acclimated fish clearly differed. Fish acclimated to 35 ppt had the highest RMR in normoxia (120–90 Torr), approximately 9 $\mu\text{mol O}_2 \text{kg}^{-1} \text{h}^{-1}$, which was about 30% greater than that for fish in the other two acclimation groups (Fig. 2D). The overall RI of the 35 ppt group was about 0.47, substantially lower than the values in the other two treatments (0.70 and 0.81 for 0 and 11 ppt, respectively), indicating a lower degree of oxyregulation at the highest salinity (Fig. 2E). This conclusion was re-enforced by the M–M analysis, which revealed the highest K_m (i.e. lowest O_2 affinity) in this group (~ 16 Torr). Notably, when acclimated to isosmotic salinity, killifish showed the lowest K_m (~ 3 Torr), denoting a much higher O_2 affinity of the whole organism (Fig. 2F). The P_{crit} exhibited a different pattern from the K_m . While the value was again lowest at 11 ppt (~ 21 Torr), it was highest at 0 ppt (~ 41 Torr) and intermediate at 35 ppt (~ 30 Torr) (Fig. 2G).

Ventilation during progressive hypoxia

Fig. 3A–C shows the effect of water P_{O_2} on the ventilation of killifish. Table 1 summarizes specific comparisons of the ventilatory responses of fish acclimated under normoxia (>90 Torr) and severe hypoxia (8–0 Torr). Ventilation increased during progressive hypoxia in all three groups and then declined at very low P_{O_2} . The P_{O_2} onset for increases in ventilation was higher in fish acclimated to 0 ppt (approximately 56 Torr) in comparison with fish acclimated to 11 and 35 ppt (approximately 22 Torr) (Fig. 3A–C). The P_{O_2} at which fish reached maximum ventilation was also higher in 0 ppt-acclimated fish (22 Torr) than in fish acclimated to 11 and 35 ppt (15 and 16 Torr, respectively) (Fig. 3A–C). Changes in amplitude contributed towards alterations in ventilatory index to a much greater extent than changes in frequency.

Overall ventilation, as captured by the ventilatory index, was significantly greater in the 0 ppt group under normoxia, and this difference from the other two treatments increased progressively under hypoxia (Fig. 3C, Table 1). This effect was almost entirely due to a greater pressure amplitude in the 0 ppt-acclimated fish under both normoxia and hypoxia (Fig. 3B, Table 1); there were no differences in ventilation frequency among salinities (Fig. 3A,

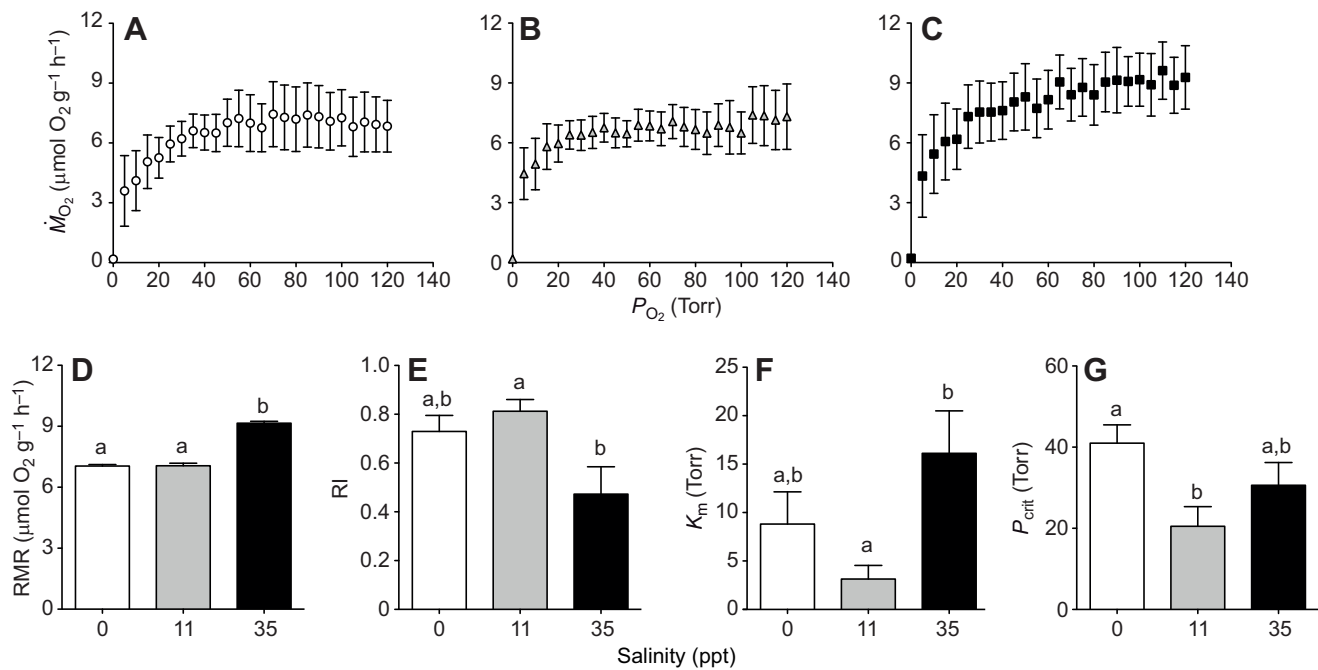


Fig. 2. Oxygen consumption rate. (A–C) Effect of water P_{O_2} on oxygen consumption rate (\dot{M}_{O_2}) of *F. heteroclitus* acclimated to 0 ppt (A), 11 ppt (B) and 35 ppt (C). (D) Routine metabolic rate (RMR), (E) regulation index (RI), (F) affinity constant (K_m) and (G) critical oxygen tension (P_{crit}) in *F. heteroclitus* exposed to progressively decreasing water P_{O_2} . Data from A–C are plotted as \dot{M}_{O_2} averages every 5 Torr. Data in D–G have been calculated on an individual fish basis. Data are means \pm s.e.m. ($n=8$). Bars sharing the same lowercase letters are not statistically different (one-way ANOVA).

Table 1). Furthermore, all ventilatory parameters were the same under both normoxia and hypoxia between 11 and 35 ppt.

Blood parameters

When blood P_{50} was determined at $P_{CO_2}=1.9$ Torr (Fig. 4A), there was an overall significant effect of oxygen, but not of salinity, and no significant interaction. In normoxia, the blood O_2 affinity (P_{50}) did not change with acclimation to different salinities (Fig. 4A). The P_{50} was significantly higher (i.e. O_2 affinity was lower) in fish exposed to hypoxia at 35 ppt compared with those exposed to normoxia (Fig. 4A), while there was no difference at the other salinities. At $P_{CO_2}=7.6$ Torr, both salinity and O_2 had significant effects, and P_{50} was overall higher both in normoxia- and in hypoxia-exposed fish compared with P_{50} at $P_{CO_2}=1.9$ Torr (Fig. 4B). There was no significant interaction effect. Interestingly, when blood from 35 ppt-acclimated fish was assayed at 7.6 Torr, there was no significant difference between normoxia and hypoxia.

There was a significant overall effect of oxygen on blood Hct. Under normoxia, blood Hct (% RBC; Fig. 4C) was around 27–30% and did not differ among salinities. Hct was significantly elevated (approximately 1.3-fold) when fish were exposed to hypoxia regardless of salinity. However, there was no overall effect of salinity in either normoxia- or hypoxia-exposed fish (Fig. 4C), and no significant interaction. Salinity had an effect on blood [Hb] (Fig. 4D). In contrast to Hct, [Hb] under normoxia was significantly greater in the 11 ppt group (about 1 mmol l^{-1}) than in the other two treatments (about 0.75 mmol l^{-1}) (Fig. 4D). [Hb] increased slightly after hypoxia exposure at all salinities, but no significant effect of oxygen was detected. Under normoxia, MCHC (Fig. 4E) did not vary across salinities. In hypoxia-exposed fish, MCHC was lower (Fig. 4E), reflecting the elevated Hct and virtually unchanged [Hb]. At 11 and 35 ppt, MCHC was significantly lower in hypoxia than in normoxia, even though there was no overall effect of oxygen.

There was no significant effect of salinity on the RBC ATP/GTP concentration ratio (Fig. 4F). The ATP/GTP ratio was lower in hypoxia-exposed fish independent of salinity; however, the effect of oxygen was only significant in 0 and 11 ppt-acclimated fish. No significant interaction was detected. Oxygen had a strong significant effect on the RBC concentrations of both ATP and GTP (Fig. 4G,H). [ATP] and [GTP] were much lower in hypoxia-exposed fish regardless of salinity acclimation; however, this effect was significant only in 0 ppt-acclimated fish. In normoxia, 0 ppt-acclimated fish had higher absolute [ATP] and [GTP] than fish acclimated to 11 and 35 ppt.

Table 2 shows the effect of equilibration to a physiological P_{CO_2} (1.9 Torr) and to a higher P_{CO_2} (7.6 Torr) on the whole-blood pH of killifish in normoxia and hypoxia. At P_{CO_2} of 1.9 Torr, oxygen had a significant overall effect, while salinity did not (Table 2). For P_{CO_2} of 7.6 Torr, there was a significant interaction between the parameters, while the separate effects of oxygen and salinity were not significant. Blood pH was consistently lower in fish exposed to hypoxia at all salinities (Table 2), and, as expected, it was lower when blood was equilibrated to a higher P_{CO_2} (7.6 Torr). At 7.6 Torr, blood from fish acclimated to 35 ppt and exposed to hypoxia had a significantly lower pH than blood from normoxia fish (Table 2).

There was a significant overall effect of oxygen, but no significant interaction between oxygen and salinity on the Bohr coefficient (Φ ; Table 2). 0 ppt-acclimated fish had the smallest Φ in normoxia (Table 2) and a large but very variable significant increase occurred in hypoxia (Table 2). Fish acclimated to 11 ppt exhibited a greater Φ under normoxia when compared with those acclimated to 0 ppt, but the increase after exposure to hypoxia was variable and not significant (Table 2). Fish acclimated to 35 ppt also did not show a significant difference between normoxia and hypoxia (Table 2). At all salinity acclimations, Φ was higher in fish exposed to hypoxia (Table 2).

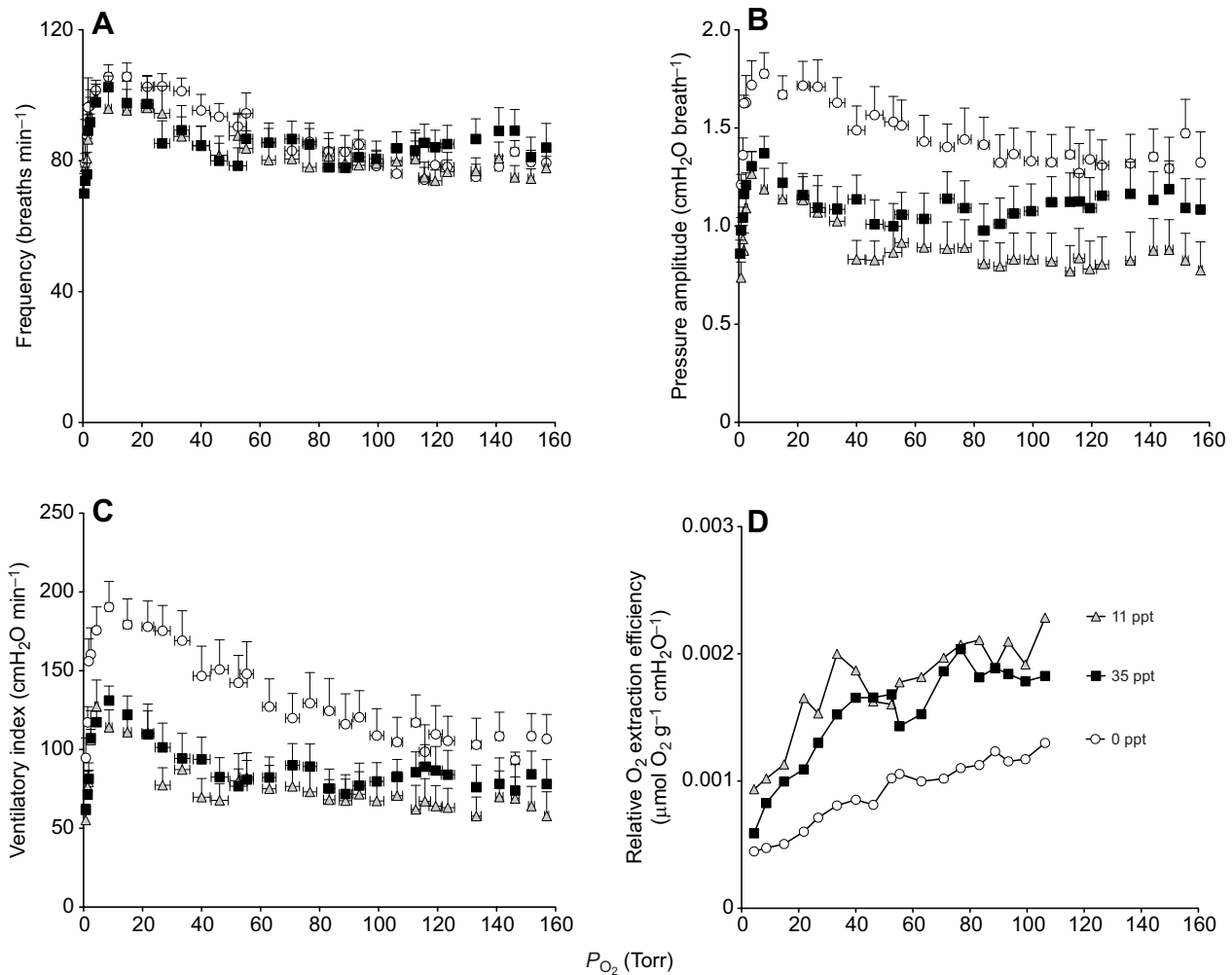


Fig. 3. Effect of P_{O_2} on ventilation in *F. heteroclitus* acclimated to 0, 11 and 35 ppt. (A) Ventilation frequency, (B) pressure amplitude, (C) ventilatory index and (D) relative extraction efficiency (\dot{M}_{O_2} /ventilatory index). Data are plotted as averages every 5 Torr. Data in D were calculated from the mean values in Figs 2A–C and 3C, therefore no s.e.m. is shown. Otherwise, data are means \pm s.e.m. ($n=11$ for A–C).

The cooperativity coefficients (Hill coefficient, n_{50}) for all treatments are summarized in Table 3. At both P_{CO_2} values tested, two-way ANOVA revealed a strong significant overall effect of oxygen, while no significant effect of salinity was detected. At P_{CO_2} of 1.9 Torr there was a significant interaction, while at P_{CO_2} of 7.6 Torr there was not. For all salinities, the Hill coefficient was higher in fish exposed to hypoxia, regardless of P_{CO_2} (Table 3). Fish

acclimated to all three salinities under normoxia showed an n_{50} lower than or close to 1 (Table 3), indicating negligible cooperativity. In turn, the highest n_{50} values were seen in fish acclimated to 0 and 11 ppt, after exposure to hypoxia, when assayed at 7.6 Torr (Table 3). At a P_{CO_2} of 1.9 Torr, a significant difference between the Hill coefficient of fish in normoxia and hypoxia at both 0 and 35 ppt was detected (Table 3). At a P_{CO_2} of 7.6 Torr, the same was observed for fish acclimated to 0 ppt (Table 3).

Table 1. Ventilatory frequency, ventilatory pressure amplitude and ventilatory index in *Fundulus heteroclitus* acclimated to a salinity of 0, 11 and 35 ppt in normoxia (>90 Torr) and in severe hypoxia (8–0 Torr)

	0 ppt	11 ppt	35 ppt
Normoxia (>90 Torr)			
Frequency (breaths min^{-1})	78.73 \pm 3.24 ^a	76.35 \pm 3.55 ^a	83.89 \pm 4.95 ^a
Amplitude (cmH ₂ O breath ⁻¹)	1.33 \pm 0.13 ^a	0.82 \pm 0.13 ^b	1.01 \pm 0.11 ^b
Index (cmH ₂ O min ⁻¹)	109.28 \pm 11.49 ^a	66.27 \pm 11.41 ^b	83.62 \pm 11.66 ^b
Hypoxia (8–0 Torr)			
Frequency (breaths min^{-1})	83.03 \pm 4.29 ^x	85.52 \pm 3.78 ^x	90.73 \pm 2.65 ^x
Amplitude (cmH ₂ O breath ⁻¹)	1.59 \pm 0.07 ^x	1.03 \pm 0.08 ^y	1.20 \pm 0.06 ^y
Index (cmH ₂ O min ⁻¹)	146.29 \pm 9.63 ^x	90.74 \pm 14.29 ^y	112.24 \pm 6.28 ^y

Data are means \pm s.e.m. ($n=11$ –12). Ventilation data sharing the same lowercase letters are not statistically different among the salinities (one-way ANOVA) within each oxygen level.

Gill morphometrics and morphology

The present morphological measurements were made only on the gills of fish under normoxia. Fig. 5A–C shows three representative histological sections of killifish gills. In fish acclimated to 0 ppt (Fig. 5A), the epithelium covering the lamellae was protuberant and thicker than in fish acclimated to 11 and 35 ppt, which showed thinner, more compact lamellae (Fig. 5B,C). Ionocytes (mitochondria-rich cells) were seen scattered throughout the length of the filament, but not on the lamellae at any of the three salinities. The ILCM (Fig. 6A) was smallest in fish acclimated to 35 ppt (about 167 μm^2), similar at 11 ppt and significantly higher by about 22% in fish acclimated to 0 ppt. There was no difference in ionocyte density between the different salinities (Fig. 6B). The ratio between the epithelial cell layer area and the lamellar height was measured as a

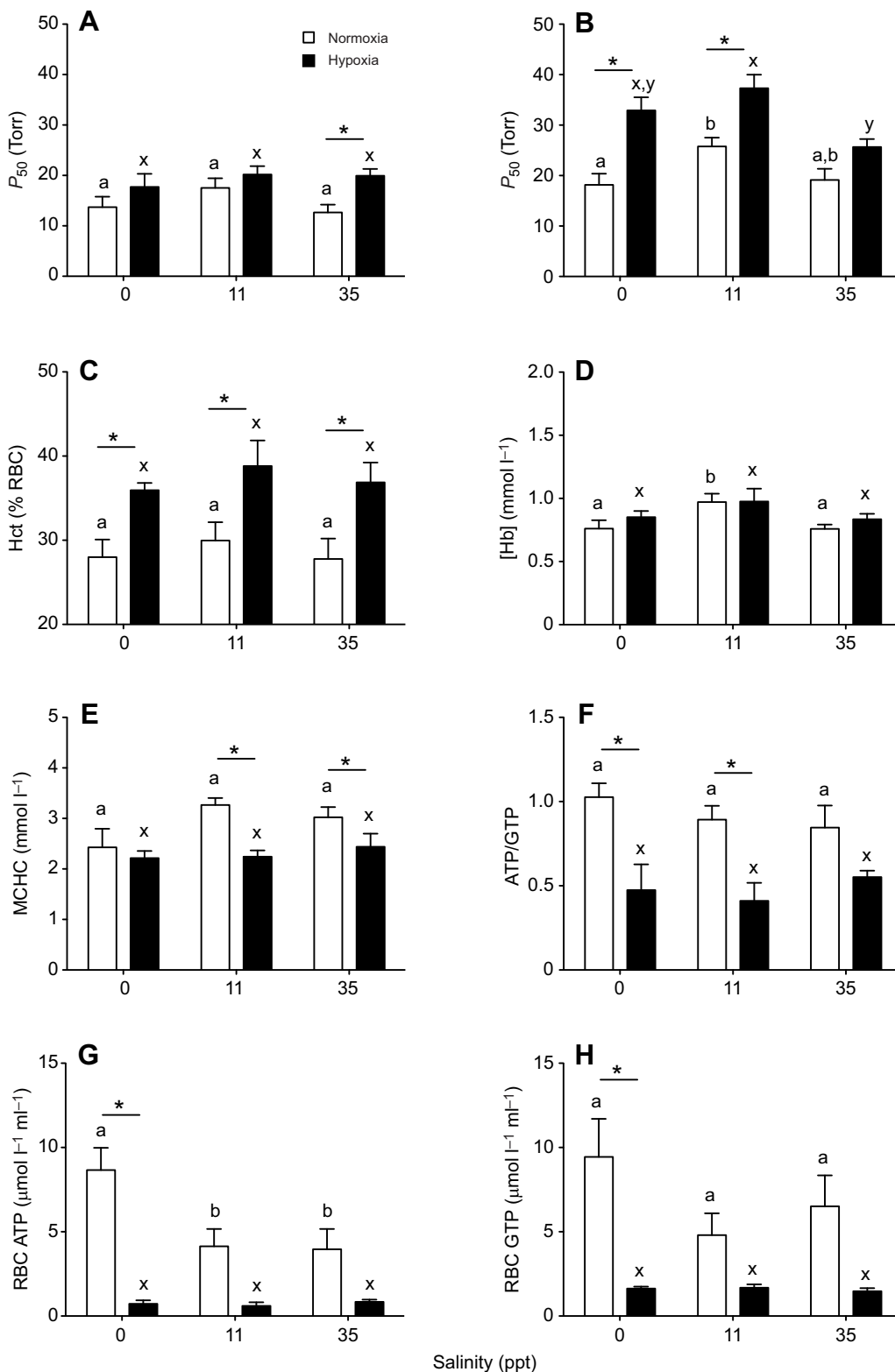


Fig. 4. Blood parameters in *Fundulus heteroclitus* acclimated to 0, 11 and 35 ppt exposed to normoxia or hypoxia. (A,B) Haemoglobin (Hb) oxygen affinity (P_{50}) assayed at P_{CO_2} of 1.9 Torr (A) and 7.6 Torr (B). (C) Hematocrit (Hct; percentage red blood cells, % RBC), (D) haemoglobin concentration ([Hb]), (E) mean cell Hb concentration (MCHC), (F) ATP/GTP ratio, (G) RBC ATP concentration and (H) RBC GTP concentration. Data are means \pm s.e.m. ($n=7$). Bars sharing the same lowercase letters are not statistically different at the same oxygen level. Asterisks indicate significant differences between normoxia and hypoxia at the same salinity (Bonferroni *post hoc* test). Two-way ANOVA P -values: P_{50} at $P_{CO_2}=1.9$ Torr: $P_{interaction}=0.4772$, $P_{oxygen}=0.0046$, $P_{salinity}=0.2153$; P_{50} at $P_{CO_2}=7.6$ Torr: $P_{interaction}=0.2447$, $P_{oxygen}<0.0001$, $P_{salinity}=0.0005$; Hct: $P_{interaction}=0.9774$, $P_{oxygen}=0.0004$, $P_{salinity}=0.6009$; [Hb]: $P_{interaction}=0.5733$, $P_{oxygen}=0.1500$, $P_{salinity}=0.0069$; MCHC: $P_{interaction}=0.5865$, $P_{oxygen}=0.0001$, $P_{salinity}=0.08610$; ATP/GTP: $P_{interaction}=0.4650$, $P_{oxygen}<0.0001$, $P_{salinity}=0.6678$; RBC ATP: $P_{interaction}=0.0622$, $P_{oxygen}<0.0001$, $P_{salinity}=0.0621$; RBC GTP: $P_{interaction}=0.4477$, $P_{oxygen}=0.0012$, $P_{salinity}=0.4479$.

proxy for the distance for gas diffusion at the lamellae (Fig. 6C). A higher ratio indicates thicker coverage of the exposed respiratory area. 0 ppt-acclimated fish had the highest ratio, which was significantly different from that of fish at 11 ppt (Fig. 6C). Fig. 6D shows the total lamellar surface area (SA_{total}) of the second gill arch in killifish. SA_{total} was lowest in fish acclimated to 0 ppt (about $6.3 \times 10^7 \mu m^2$), and significantly different from SA_{total} at the

other two salinities (Fig. 6D). SA_{total} did not change between 11 and 35 ppt. Table 4 summarizes the effects of salinity acclimation on the quantitative metrics of gill morphology. 11 ppt-acclimated fish had longer filaments, a higher number of lamellae per filament, a higher number of filaments on the 2nd gill arch and a higher SA_{FL} (Table 4), although these were not statistically significant.

Table 2. Whole-blood pH at physiological or high P_{CO_2} and Bohr coefficient (Φ) of *F. heteroclitus* acclimated to 0, 11 and 35 ppt in normoxia or exposed to hypoxia

	Salinity (ppt)	Physiological P_{CO_2}		High P_{CO_2}	
		Normoxia	Hypoxia	Normoxia	Hypoxia
Whole-blood pH	0	7.53±0.08 ^a	7.35±0.05 ^{x,y}	7.18±0.07 ^a	7.18±0.06 ^{x,y}
	11	7.48±0.07 ^a	7.45±0.04 ^x	7.28±0.05 ^a	7.20±0.03 ^x
	35	7.48±0.06 ^a	7.16±0.07 ^{y,*}	7.26±0.08 ^a	6.96±0.10 ^{y,*}
Bohr coefficient (Φ)	0	-0.75±0.09 ^a		-4.47±1.23 ^{x,*}	
	11	-1.08±0.39 ^a		-2.71±0.78 ^{x,y}	
	35	-1.14±0.19 ^a		-1.43±0.30 ^y	

Whole-blood pH is given at physiological P_{CO_2} (1.9 Torr) and high P_{CO_2} (7.6 Torr). Data are means±s.e.m. ($n=6-8$). Means sharing the same lowercase letters are not statistically different at the same oxygen level. Asterisks indicate significant differences between normoxia and hypoxia at the same salinity (Bonferroni *post hoc* test). Two-way ANOVA P -values: $P_{\text{CO}_2}=1.9$ Torr: $P_{\text{interaction}}=0.1812$, $P_{\text{oxygen}}=0.0064$, $P_{\text{salinity}}=0.1438$; $P_{\text{CO}_2}=7.6$ Torr: $P_{\text{interaction}}=0.0457$, $P_{\text{oxygen}}=0.0984$, $P_{\text{salinity}}=0.1785$; Φ : $P_{\text{interaction}}=0.0300$, $P_{\text{oxygen}}=0.0004$, $P_{\text{salinity}}=0.1265$. Blood pH comparisons in normoxia and hypoxia were only performed within a single P_{CO_2} .

DISCUSSION

Overview

Our ultimate goal was to determine the relationship between salinity acclimation and whole-animal respiratory capacity in the euryhaline killifish *F. heteroclitus* and to elucidate the mechanisms by which salinity may influence hypoxia tolerance. Our study tested three hypotheses. Firstly, our data partially support the hypothesis based

on energetic considerations that *F. heteroclitus* acclimated to the isosmotic salinity (~11 ppt) would exhibit highest hypoxia tolerance. Secondly, we confirmed the hypothesis that in order to acclimate to FW, killifish compromised gill respiratory capacity by adopting the lowest lamellar surface area and highest ILCM, resulting in lower effective permeability for O_2 . Thirdly, we confirmed that physiological adjustments were made in light of the

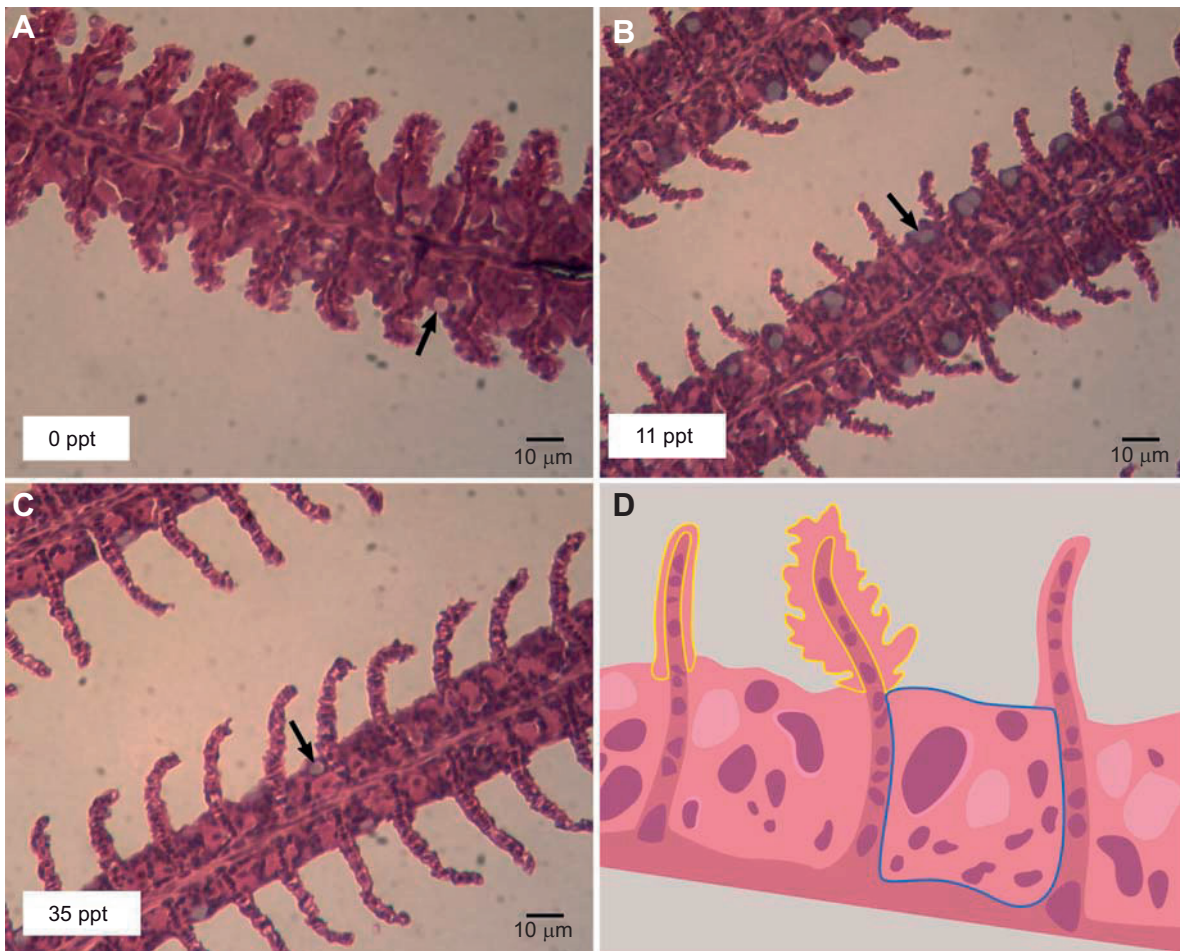


Fig. 5. Histological sections of *F. heteroclitus* gill filaments acclimated to different salinities in normoxia. (A) 0 ppt, (B) 11 ppt and (C) 35 ppt. (D) Illustration of gill filament detailing how morphological analysis was performed. Black arrows indicate ionocytes. In 0 ppt-acclimated fish, the epithelial cell layer covering the lamella is bulging and thicker than in 11 and 35 ppt-acclimated fish. Epithelial cell coverage (Fig. 6C) was measured as outlined in yellow in D. The interlamellar cell mass (ILCM) is visible in all three salinities and highlighted in blue in D.

Table 3. Hill cooperativity coefficient (n_{50}) in whole blood of *F. heteroclitus* acclimated to 0, 11 and 35 ppt in normoxia or exposed to hypoxia, assayed at P_{CO_2} of 1.9 or 7.6 Torr

Salinity (ppt)	n_{50}			
	Physiological P_{CO_2}		High P_{CO_2}	
	Normoxia	Hypoxia	Normoxia	Hypoxia
0	0.91±0.03 ^a	1.21±0.08 ^{x,*}	1.12±0.03 ^a	1.35±0.03 ^{x,*}
11	1.02±0.07 ^{a,b}	1.03±0.03 ^y	1.09±0.04 ^a	1.23±0.03 ^{x,y}
35	0.78±0.03 ^b	1.04±0.05 ^{x,y,*}	1.09±0.03 ^a	1.13±0.05 ^y

Physiological P_{CO_2} =1.9 Torr; high P_{CO_2} =7.6 Torr. Data are means±s.e.m. ($n=6-8$). Means sharing the same lowercase letters are not statistically different at the same oxygen level. Asterisks indicate significant differences between normoxia and hypoxia at the same salinity (Bonferroni *post hoc* test). Two-way ANOVA P -values: P_{CO_2} =1.9 Torr: $P_{interaction}=0.0041$, $P_{oxygen}<0.0001$, $P_{salinity}=0.0241$; P_{CO_2} =7.6 Torr: $P_{interaction}=0.1329$, $P_{oxygen}=0.0003$, $P_{salinity}=0.0264$. Normoxia and hypoxia data were only compared within a single P_{CO_2} .

osmorepiratory compromise, where FW-acclimated fish had the highest ventilatory indices in normoxia and hypoxia. This could be an indication of compensation for the apparent reduced gill permeability and the need for higher ventilatory work in order to maintain satisfactory O_2 uptake at the gills. Overall, we conclude that many differences in the O_2 transport cascade are associated with the osmorepiratory compromise in killifish, and that acclimation to 11 ppt is the most advantageous and acclimation to 0 ppt is the most challenging for respiratory gas exchange.

Effects of salinity on time to LOE

Hypoxia tolerance in killifish was altered by salinity acclimation over a wide range, representative of their natural distribution in estuarine and salt marsh ecosystems (Griffith, 1974). We hypothesized that

acclimation to the salinity corresponding to the isosmotic point would yield the greatest hypoxia tolerance, as energy allocated to ionoregulation and osmoregulation would be lower. Our follow-up prediction was that hypoxia tolerance would decrease in FW and full-strength SW. To our knowledge, this is the first study to look at time to LOE in killifish in FW, where hypoxia tolerance was 85% lower in comparison to that at 11 ppt. The 11 ppt group showed the highest time to LOE in hypoxia, but there was no significant difference between fish acclimated at 11 and 35 ppt (Fig. 1), contrary to our prediction based on the energetic costs of ionoregulation and osmoregulation in SW. Previously, we evaluated time to LOE at a common assay salinity of 11 ppt in fish that had been acclimated to 0, 11 and 35 ppt (data not shown) in order to evaluate whether the exposure or the acclimation salinity was of greater influence. No differences in time to LOE were observed between fish that were tested at their respective acclimation salinity and those tested at 11 ppt, reinforcing the idea that the acclimation salinity is likely to be responsible for alterations in hypoxia tolerance.

Loss of the ability to maintain position in the water column and unresponsiveness to stimuli threatens survival in the wild. Therefore, the time required to reach such an endpoint is an important ecological indicator of tolerance to hypoxia (Mandic et al., 2012). While the mechanisms underlying such a loss of function are still poorly understood, the inability to supply ATP to the brain may underlie the patterns of LOE in fishes (Mandic et al., 2012).

Times to LOE reported here are well above values found in the literature for *F. heteroclitus* (Borowiec et al., 2015; McBryan et al., 2016). For example, killifish acclimated to 20 ppt and 15°C had a time to LOE of 75 min at 3 Torr (McBryan et al., 2016), versus 11 h reported here for fish at 15 ppt and 3.5 Torr (18°C), highlighting that small differences in methodology could result in large differences in time to LOE.

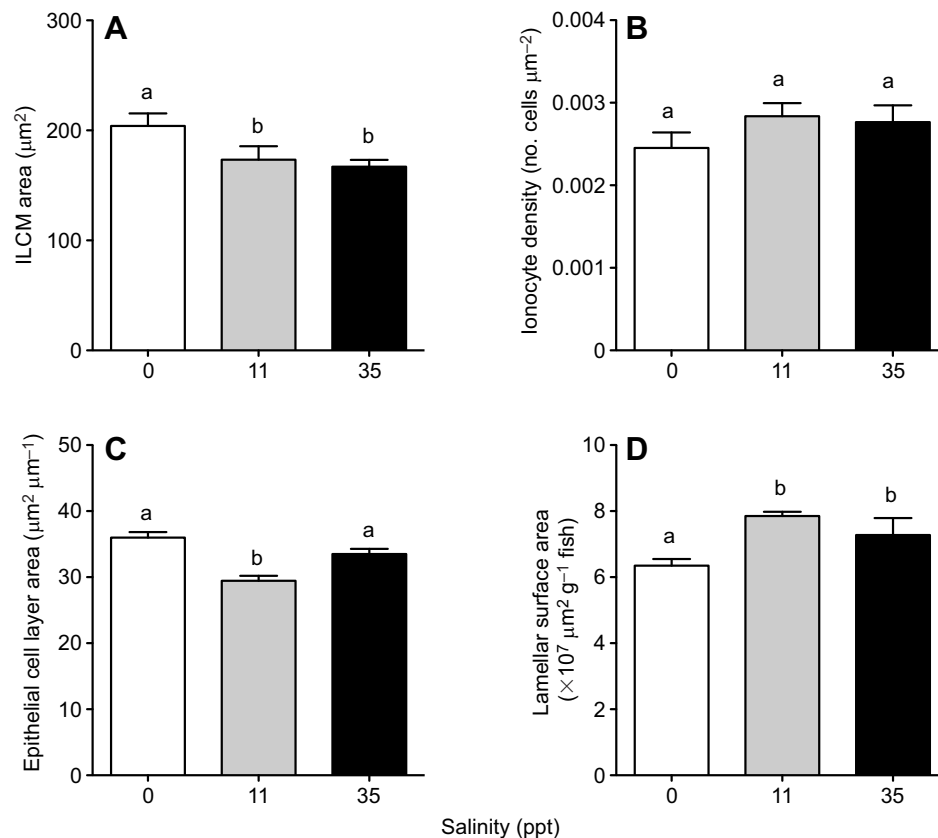


Fig. 6. Effect of salinity on gill morphometrics of the second gill arch in *F. heteroclitus* in normoxia. (A) ILCM area, (B) ionocyte density, (C) epithelial cell coverage of the lamellae and (D) lamellar surface area. Data are means±s.e.m. ($n=6$). Bars sharing the same lowercase letters are not statistically different (one-way ANOVA).

Table 4. Gill morphometrics in *F. heteroclitus* acclimated to 0, 11 and 35 ppt in normoxia

Morphometrics	0 ppt	11 ppt	35 ppt
Lamellar height (μm)	43.89 \pm 0.67 ^a	44.32 \pm 2.76 ^a	45.08 \pm 3.33 ^a
Lamellar width (μm)	17.68 \pm 0.69 ^a	16.73 \pm 0.35 ^a	16.42 \pm 0.47 ^a
Filament length (mm)	1.56 \pm 0.05 ^a	1.60 \pm 0.03 ^a	1.51 \pm 0.06 ^a
Lamellar frequency (lamellae mm ⁻¹)	25.37 \pm 1.12 ^a	26.33 \pm 0.83 ^a	25.24 \pm 0.75 ^a
SA _{FL} ($\times 10^6 \mu\text{m}^2$)	1.38 \pm 0.08 ^a	1.58 \pm 0.09 ^a	1.40 \pm 0.10 ^a
Number filaments in 2nd gill arch	47.66 \pm 0.96 ^a	50.66 \pm 0.93 ^a	47.16 \pm 1.51 ^a

SA_{FL}, filamental lamellar surface area. Data are means \pm s.e.m. ($n=5-6$).

Morphometrics data sharing the same lowercase letters are not statistically different among the salinities (one-way ANOVA). Different parameters were not compared.

Effects of salinity on respiratory responses to hypoxia

It has been hypothesized that metabolic rates of fishes should reflect changes associated with osmoregulatory costs (Zadunaisky, 1984). A number of studies have attempted to quantify the amount of energy allocated towards ionoregulation, but different methodologies yielded varying results (Kirschner, 1995; Potts, 1954; Boeuf and Payan, 2001). Theoretical calculations have placed the cost of ion transport at only 0.5–1% of resting \dot{M}_{O_2} (McCormick et al., 1989), while direct measurements have yielded values as high as 27% (Rao, 1968). In *F. heteroclitus*, Kidder et al. (2006a) estimated the cost as 6–10% in SW, and lower in FW, based on the higher ionic and osmotic gradients from water to blood in SW. Measurements of \dot{M}_{O_2} in isolated gill preparations in cutthroat trout (*Oncorhynchus clarki clarki*) suggested that NaCl gill transport represents less than 4% of the whole animal's energy budget in FW and SW (Morgan and Iwama, 1999). Therefore, despite the uncertainties in the empirical and theoretical data, osmoregulatory costs may occupy an important share of the animal's energy budget.

Our first hypothesis was that the isosmotic salinity would result in lower osmoregulatory costs and therefore the lowest routine \dot{M}_{O_2} (RMR). Instead, we saw no differences in RMR in fishes acclimated to 0 and 11 ppt, and the greatest RMR in fishes acclimated to 35 ppt (Fig. 2D). This higher RMR at 35 ppt agrees qualitatively with the theoretical prediction of Kidder et al. (2006a). However, in contrast to the present data and to their own prediction based on theory, in a different study, Kidder et al. (2006b) saw no differences in RMR of *F. heteroclitus* acclimated to either FW, SW and 10 ppt. The authors suggested that differential ionoregulatory costs were hidden by adjustment of other expenditures. In two additional species of euryhaline fishes, *Galaxias maculatus* (Urbina and Glover, 2015) and *Sciaenops ocellatus* (Ern and Esbaugh, 2018), no differences in RMR were observed among fish acclimated to a wide salinity range.

Any environmental factor that has the potential to influence O_2 demand is likely to have implications for whole-animal O_2 uptake and, consequently, hypoxia tolerance. P_{crit} , a common predictor of hypoxia tolerance, is the O_2 level below which the animal can no longer sustain a constant rate of oxygen uptake (oxyregulation); below that, uptake becomes a function of environmental O_2 availability (oxyconformation). P_{crit} has been widely used as an indication of the degree of a species' hypoxia tolerance (e.g. Mandic et al., 2009; Rogers et al., 2016). However, recent studies have pointed to the impracticality of translating P_{crit} values into the real world, and have challenged its actual significance as a hypoxia tolerance trait (Mueller and Seymour, 2011; Wood, 2018). Therefore, in our study, we analysed the \dot{M}_{O_2} versus P_{O_2} relationships using the

framework proposed by Alexander and McMahon (2004) and Mueller and Seymour (2011), where a non-linear function is used to describe the P_{O_2} versus \dot{M}_{O_2} plots (Marshall et al., 2013). The analysis of the ability to regulate \dot{M}_{O_2} over a range of P_{O_2} values (the RI) reveals the degree to which \dot{M}_{O_2} is maintained independently of environmental P_{O_2} .

Fish acclimated to 35 ppt had the lowest RI, with a pattern closer to oxyconformation than at 11 or 0 ppt (Fig. 2E). Blewett et al. (2013) identified *F. heteroclitus* as an oxyconforming species, contrasting with the results of several other studies including the present one. However, Blewett et al. (2013) similarly found the highest \dot{M}_{O_2} during hypoxia in killifish at intermediate salinity (16 ppt), despite the pattern of oxyconformation in their study. The summary of Wood (2018) indicates a great diversity of response patterns reported for this species (see below). Fish acclimated to 11 ppt showed a greater ability to regulate \dot{M}_{O_2} down to very low P_{O_2} values, as reflected in the higher RI, lower K_m and lower P_{crit} values (Fig. 2E–G). K_m represents the affinity constant derived from the M–M function (Marshall et al., 2013).

There is an influence of salinity on the \dot{M}_{O_2} responses to declining P_{O_2} . We calculated P_{crit} using the greatest difference method (Mueller and Seymour, 2011) and, to our knowledge, this is the first report of either a P_{crit} or a description of the relationship between \dot{M}_{O_2} and P_{O_2} for killifish acclimated to FW (Fig. 2A,G). The P_{crit} values reported here lie within the broad range of values reported for *F. heteroclitus* at other salinities, and our value for 11 ppt-acclimated killifish (20 Torr) is the lowest reported so far. An early study by Cochran and Burnett (1996) found a P_{crit} of 35 Torr at 30°C in 'seawater', although no precise value of salinity was reported. Richards et al. (2008), using fish acclimated to 10 ppt, measured a P_{crit} of 63 Torr, while both McBryan et al. (2016) and Borowiec et al. (2015) measured a P_{crit} of 39 Torr, with fish acclimated to 20 and 4 ppt, respectively. We observed that the onset of significant increases in ventilation occurred at a P_{O_2} of about 15 Torr higher than the measured P_{crit} in fish acclimated to 0 ppt, while in fish at 11 and 35 ppt, P_{crit} coincided with the onset of increases in ventilation. Additionally, we noted that the onset of a decline in ventilation in hypoxia occurred at P_{O_2} values below the measured P_{crit} for all three salinities. This indicates that even at P_{O_2} below that often considered to be the threshold for the onset of anaerobic metabolism, elevated ventilation (an energetically expensive activity) is maintained.

We used fish of similar sizes across salinities as a way of standardizing the rate of P_{O_2} decline across treatments, as recommended by Regan and Richards (2017). CO_2 accumulation is another concern when using closed-system respirometry, because of the associated decrease in water pH. Many but not all studies have reported no effect of P_{CO_2} on P_{crit} (reviewed by Rogers et al., 2016) and indeed Cochran and Burnett (1996) reported a lack of effect of P_{CO_2} on *F. heteroclitus* P_{crit} . However, the latter investigation was performed in 'seawater', and it is important to consider that at 0 ppt the water buffering capacity would be lower and therefore any effects of CO_2 on pH could be magnified.

Effects of salinity on ventilatory responses to hypoxia

In hypoxia, the majority of species increase ventilation mainly through increases in stroke volume rather than through increases in ventilation frequency, as this strategy is more energetically favourable (Perry, 2011). In normoxia, fish acclimated to 0 ppt exhibited a higher ventilatory index, driven by the ventilation amplitude, as there were no differences in ventilation frequency. This pattern of higher ventilatory index at 0 ppt became accentuated during progressive hypoxia. At a P_{O_2} of about 56 Torr, the

ventilatory index of 0 ppt-acclimated fish started to deviate from those at the other salinities. However, there were no differences in the two components of the ventilatory index (frequency and amplitude) between fish acclimated to 11 and 35 ppt (Fig. 3C). It is clear that fish acclimated to 0 ppt must put higher energetic work into ventilation in order to achieve comparable levels of \dot{M}_{O_2} during normoxia, and to an even greater extent during hypoxia.

We estimated the relative oxygen extraction efficiency by dividing \dot{M}_{O_2} by the ventilatory index (Fig. 3D). In comparison to fish acclimated to 11 and 35 ppt, 0 ppt-acclimated fish showed a lower extraction efficiency throughout the entire P_{O_2} range. Although the low extraction efficiency may help explain the high K_m and P_{crit} values seen in 0 ppt-acclimated fish, the lack of difference between 11 and 35 ppt groups does not fully explain the higher regulation capacity seen in fish acclimated to 11 ppt.

As ventilation is thought to be energetically costly (Perry et al., 2009), at about 5–15% of RMR (Cameron and Cech, 1970), we speculate that the lower hypoxia tolerance observed in FW fish could be, at least in part, a reflection of the higher energy expenditure for ventilation. However, a recent examination (Ern and Esbaugh, 2018) of the effects of salinity acclimation (0–60 ppt) on ventilation in the euryhaline red drum (*Sciaenops ocellatus*) saw no effect of salinity on gill ventilation, contrary to our data.

Effects of salinity on gill morphometrics and morphology

We observed no differences in ionocyte density between fish acclimated to the three salinities (Fig. 6B). In a previous study on *F. heteroclitus*, Katoh and Kaneko (2003) observed a significant decrease in ionocyte density 3 days after transfer from SW to FW, but after fish were kept at those salinities, these differences disappeared. The disparity in hypoxia tolerance indices reported for *F. heteroclitus* could also be a function of the morphological adjustments that happen at the gills when fish are acclimated to different salinities. We observed that 0 ppt-acclimated killifish had a smaller lamellar surface area in relation to that of fish at 11 and 35 ppt. Furthermore, 0 ppt-acclimated fish had thicker lamellae in addition to a thicker epithelial cell layer and a greater ILCM that was greater than observed in 11 and 35 ppt-acclimated fish (Fig. 6A). As gas diffusion at the lamellae is related to the thickness of the water-to-blood barrier (Evans et al., 2005), any increases in this distance have the potential to impair whole-animal gas transfer (reviewed by Perry, 1998). Rainbow trout (*Oncorhynchus mykiss*) acclimated to ion-poor water dramatically increased ionocyte proliferation and coverage of the lamellae (Greco et al., 1996), resulting in a reduction in hypoxia tolerance (Thomas et al., 1988). In turn, freshwater adaptation in prickly sculpin (*Cottus asper*) was associated with thicker gills and a decrease in respiratory surface area, resulting in a higher P_{crit} (Henriksson et al., 2008). Our morphological data do not support the hypothesis that the same might be happening to the freshwater killifish, as we did not observe ionocytes on the lamellae at any salinity (Fig. 5). However, we observed an increase in the thickness and size of the epithelial cell layer covering the lamellae, indicative of hypertrophy and/or hyperplasia (Mallatt, 1985). Additionally, the ILCM partially occluding the water channels (Fig. 6A) was larger in fish acclimated to 0 ppt than fish in SW, contributing to the reduction in respiratory surface area and an apparent decrease in gas permeability.

Since the ILCM was first reported (Sollid et al., 2003), many studies have looked at how different environmental factors can alter the ILCM in a variety of fish species (Nilsson, 2007; Mitrovic and Perry, 2009; LeBlanc et al., 2010; Nilsson et al., 2012; Blair et al., 2016). In light of the known ability of several species, including

F. heteroclitus, to quickly increase the respiratory surface when oxygen demand is high, via the retraction or sloughing of the ILCM (Barnes et al., 2014; McBryan et al., 2016), it will be of interest in future studies to examine gill morphology of killifish under hypoxia. A few studies have looked at the direct influence of salinity on the ILCM. In the mangrove killifish (*Kryptolebias marmoratus*), the ILCM decreased in animals acclimated to hypersaline conditions in comparison with FW (LeBlanc et al., 2010). The Arctic grayling (*Thymallus arcticus*), a freshwater salmonid, experienced a growth in ILCM when transferred to salt water, drastically reducing the gill respiratory surface (Blair et al., 2016). Similar to our results, Gibbons et al. (2018) observed an increase in ILCM area in response to a decrease in salinity, probably associated with freshwater adaptation, in threespine stickleback (*Gasterosteus aculeatus*). However, contrasting with the present investigation, none of these earlier studies examined the possible correlation between ILCM and respiratory capacity. The morphological evidence presented here suggests that the decrease in total respiratory surface area and the presence of a greater ILCM contribute to the elevated ventilatory work together with a marked reduction in hypoxia tolerance when killifish are acclimated to FW.

Effects of salinity on blood oxygen transport

We had hypothesized that changes in the respiratory surface area due to salinity acclimation would be reflected in functional changes in the blood O_2 transport characteristics. The whole-blood OEC of *F. heteroclitus* under normoxia resembles OECs from other hypoxia-tolerant fish; relatively high O_2 affinity (low P_{50}) and a low cooperativity (Hill coefficient ~ 1) are thought to improve O_2 uptake at the gills (Wells, 2009). Conversely, a high Bohr coefficient is thought to improve O_2 unloading at tissues. Our Bohr coefficients were calculated over a narrow pH range, as pH changes between low and high P_{CO_2} were fairly small, particularly in hypoxia, and therefore must be interpreted with caution. The pH values measured in our study fall within the predicted range for variations in pH with temperature, and are comparable with data from DiMichele and Powers (1982).

Upon exposure to hypoxia, we observed an increase in whole-blood P_{50} , regardless of salinity acclimation and P_{CO_2} equilibration (Fig. 4A,B), and at least at 35 ppt, blood pH declined significantly in hypoxia (Table 3). Additionally, the Hill coefficient also increased for all salinities (at both P_{CO_2} values) in hypoxia-exposed fish (Table 3), indicating an increase in cooperativity of the Hb, where the reduced O_2 affinity (i.e. higher P_{50}) favours O_2 unloading at the tissues (Wells, 2009). In hypoxia, where the O_2 supply for aerobic energy production becomes limited, fish can resort to anaerobic pathways to obtain energy, often leading to the accumulation of lactate, a response common to several fish species, including *F. heteroclitus* (Cochran and Burnett, 1996; Kraemer and Schulte, 2004). The dissociation of protons from lactate, as well as the release of protons from ATP breakdown (Hochachka and Mommsen, 1983), can cause a generalized acidosis, enhancing the Bohr effect in order to favour O_2 unloading from the Hb to the tissues, resulting in the higher P_{50} seen in fish exposed to hypoxia. Blood pH decreased in all treatments in whole blood equilibrated with a P_{CO_2} of 7.6 Torr, relative to the lower P_{CO_2} (Table 2).

The main erythrocyte organic phosphate compounds found in fish are adenosine and guanosine triphosphates (ATP, GTP), which decrease the Hb affinity for oxygen (Val, 2000). *Fundulus heteroclitus* is highly susceptible to organic phosphate allosteric modifications on Hb O_2 affinity (Greaney and Powers, 1978). The higher level of both compounds in 0 ppt-acclimated killifish

(Fig. 4G,H) is of unknown origin but may be one of several factors contributing to problems with gill O₂ uptake in FW. However, the considerable fall in ATP and GTP at all salinities during hypoxia, perhaps as a consequence of net metabolic consumption during oxygen shortage, would clearly be helpful in protecting the O₂ affinity of the blood in the face of hypoxia-associated metabolic acidosis. Thus, allosteric regulation by RBC organic phosphates may play an important role in modifying blood O₂ affinity in the face of variations in salinity, environmental O₂ levels and blood pH (Fig. 4).

Blood P_{50} values reported here (12.6 to 17.5 Torr) under normoxia are higher than previously reported for *F. heteroclitus* O₂ binding affinity (Fig. 4A,B). DiMichele and Powers (1982) working with blood from *F. heteroclitus* identified a P_{50} of around 5 Torr (at 25°C and pH 7.4), though P_{CO_2} of the blood was apparently 0 Torr. Chung et al. (2017) measured a P_{50} of 3.7 Torr while working on RBCs that had been isolated and re-suspended in HCO₃⁻-free, Hepes buffer at 15°C, pH 7.8, P_{CO_2} =0 Torr. Noteworthy, whole blood carries different elements that have the potential to alter O₂ binding affinity. These include other ions, most importantly HCO₃⁻, allosteric modifiers, buffers (plasma proteins) and probably metabolic end products such as protons and lactate. This lack of a plasma environment, as well as the known effects of Hepes in interfering with HCO₃⁻ transport (Hanrahan and Tabcharani, 1990) may alter the blood O₂ binding characteristics. It is not clear whether the values reported here are higher exclusively as a result of low pH or the use of whole blood, or whether other factors might be playing a role.

Upon hypoxia exposure, we observed a significant increase in Hct independent of salinity acclimation. The increases in MCHC accompanied by no change in [Hb] in fish acclimated to 11 and 35 ppt probably indicate a swelling of the RBCs (Fig. 4D,E). This could be beneficial for O₂ uptake at the gills, as a higher surface area of the RBC per unit of Hb would mean higher contact area at the lamellae, and a higher diffusion rate of ambient O₂ into the RBC. Additionally, β-adrenergic stimulation of RBC swelling leading to increased intracellular pH and Hb dilution, both of which increase Hb O₂ affinity, is a well-known mechanism in teleost RBCs (Nikinmaa and Huestis, 1984). β-Adrenergic stimulation of RBC membrane transporters is also present in *F. heteroclitus* (Dalessio et al., 1991). The same response was not observed in fish acclimated to 0 ppt. The lack of RBC swelling in 0 ppt-acclimated killifish could be considered as another negative aspect of FW acclimation (Fig. 4E). Taken altogether, our data suggest that the mechanisms for increasing overall O₂ carrying capacity of the blood differ among salinity acclimations.

Concluding remarks

We have shown that salinity acclimation has marked effects on the response to hypoxia in the euryhaline *F. heteroclitus*. In a recent comprehensive review, Rogers et al. (2016) identified a strong correlation between salinity and respiratory responses in water-breathing fishes. *Fundulus heteroclitus* inhabits salt marshes, which are highly dynamic environments, where they occupy deeper, more temperature stable areas in the winter, and move to shallower, lower salinity areas in the summer (Taylor et al., 1979). It has been experimentally shown that *F. heteroclitus* actively seeks different salinities based on their physiological and ecological needs (Bucking et al., 2012; Marshall et al., 2016), where in normoxia, killifish prefer salinities around 20 ppt (Fritz and Garside, 1974; Bucking et al., 2012). One could predict that in hypoxia, killifish would seek isosmotic salinities in order to alleviate the energetic needs of osmoregulation. It could also be hypothesized that unless attracted by opportunities to increase feeding or avoid predation,

killifish would avoid 0 ppt water because of the compromise between osmoregulation and respiratory capacity, evidenced by the present study.

Acknowledgements

We thank Phillip Morrison for his invaluable assistance with OEC measurement and construction, Dr Matthew Reagan for his help with gill morphometrics and Jacelyn Shu for the careful gill illustration shown in Fig. 4D. Also, thanks to Vinicius Azevedo and Dr Giorgi Dal Pont for logistic assistance.

Competing interests

The authors declare no competing or financial interests.

Author contributions

Conceptualization: M.G., P.M.S., C.W.; Methodology: M.G., H.J.B., A.L.V.; Formal analysis: M.G., H.J.B., A.L.V.; Investigation: M.G.; Writing - original draft: M.G.; Writing - review & editing: M.G., H.J.B., A.L.V., P.M.S., C.W.; Supervision: P.M.S., C.W.; Project administration: P.M.S., C.W.; Funding acquisition: P.M.S., C.W.

Funding

This study was supported by Natural Sciences and Engineering Research Council of Canada (NSERC) Discovery Grants to C.M.W. (RGPIN-2017-03843, RGPIN/473-2012) and P.M.S. (RGPIN-203189). M.G. was supported by a 4-year graduate fellowship from the University of British Columbia. A.L.V. received a Research Fellowship from Conselho Nacional de Desenvolvimento Científico e Tecnológico (CNPq) and an NSERC Canada Graduate scholarship to H.J.B.

References

- Alexander, J. E., Jr. and McMahon, R. F. (2004). Respiratory response to temperature and hypoxia in the zebra mussel *Dreissena polymorpha*. *Comp. Biochem. Physiol. A* **137**, 425-434. doi:10.1016/j.cbpb.2003.11.003
- Barnes, K. R., Cozzi, R. R. F., Robertson, G. and Marshall, W. S. (2014). Cold acclimation of NaCl secretion in a eurythermic teleost: mitochondrial function and gill remodeling. *Comp. Biochem. Physiol. A* **168**, 50-62. doi:10.1016/j.cbpa.2013.11.004
- Bartlett, G. R. (1978). Water-soluble phosphates of fish red cells. *Can. J. Zool.* **56**, 870-877. doi:10.1139/z78-120
- Blair, S. D., Matheson, D., He, Y. and Goss, G. G. (2016). Reduced salinity tolerance in the Arctic grayling (*Thymallus arcticus*) is associated with rapid development of a gill interlamellar cell mass: implications of high-saline spills on native freshwater salmonids. *Conserv. Physiol.* **4**, 1-11. doi:10.1093/conphys/cow010
- Blewett, T. A., Robertson, L. M., MacLatchy, D. L. and Wood, C. M. (2013). Impact of environmental oxygen, exercise, salinity, and metabolic rate on the uptake and tissue-specific distribution of 17α-ethynylestradiol in the euryhaline teleost *Fundulus heteroclitus*. *Aquat. Toxicol.* **138-139**, 43-51. doi:10.1016/j.aquatox.2013.04.006
- Boeuf, G. and Payan, P. (2001). How should salinity influence fish growth? *Comp. Biochem. Physiol. C* **130**, 411-423. doi:10.1016/S1532-0456(01)00268-X
- Borowiec, B. G., Darcy, K. L., Gillette, D. M. and Scott, G. R. (2015). Distinct physiological strategies are used to cope with constant hypoxia and intermittent hypoxia in killifish (*Fundulus heteroclitus*). *J. Exp. Biol.* **218**, 1198-1211. doi:10.1242/jeb.114579
- Boutlier, R. G., Heming, T. A. and Iwama, G. K. (1984). Appendix: Physicochemical parameters for use in fish respiratory physiology. In *Fish Physiology*, Vol. 10A (ed. W. S. Hoar and D. Randall), pp. 403-430. Orlando, FL: Academic Press.
- Bucking, C., Wood, C. M. and Grosell, M. (2012). Diet influences salinity preference of an estuarine fish, the killifish *Fundulus heteroclitus*. *J. Exp. Biol.* **215**, 1965-1974. doi:10.1242/jeb.061515
- Burnett, K. G., Bain, L. J., Baldwin, W. S., Callard, G. V., Cohen, S., Di, R. T., Evans, D. H., Gómez-chiarri, M., Hahn, M. E., Cindi, A. et al. (2007). *Fundulus* as the premier teleost model in environmental biology: opportunities for new insights using genomics. *Comp. Biochem. Physiol. D* **2**, 257-286. doi:10.1016/j.cbd.2007.09.001
- Cameron, J. N. and Cech, J. J. (1970). Notes on the energy cost of gill ventilation in teleosts. *Comp. Biochem. Physiol.* **34**, 447-455. doi:10.1016/0010-406X(70)90184-2
- Chung, D. J., Morrison, P. R., Bryant, H. J., Jung, E., Brauner, C. J. and Schulte, P. M. (2017). Intraspecific variation and plasticity in mitochondrial oxygen binding affinity as a response to environmental temperature. *Sci. Rep.* **7**, 1-10. doi:10.1038/s41598-017-16598-6
- Cochran, R. E. and Burnett, L. E. (1996). Respiratory responses of the salt marsh animals *Fundulus heteroclitus*, *Leiostomus xanthurus*, and *Palaemonetes pugio* to environmental hypoxia and hypercapnia and to the organophosphate pesticide, azinphosmethyl. *J. Exp. Mar. Bio. Ecol.* **195**, 125-144. doi:10.1016/0022-0981(95)00102-6
- Dalessio, P. M., DiMichele, L. and Powers, D. A. (1991). Adrenergic effects on the oxygen affinity and pH of cultured erythrocytes and blood of the mummichog,

- Fundulus heteroclitus*. *Physiol. Zool.* **64**, 1407-1425. doi:10.1086/physzool.64.6.30158222
- Díaz, R. J. and Breitburg, D. L.** (2011). The expanding hypoxic environment. In *Encyclopedia of Fish Physiology* (ed. A. P. Farrell), pp. 1746-1750. San Diego, CA: Academic Press.
- DiMichele, L. and Powers, D. A.** (1982). Physiological basis of swimming endurance between LDH-B genotypes in *Fundulus heteroclitus*. *Science* **216**, 1014-1016. doi:10.1126/science.7079747
- Edwards, S. L. and Marshall, W. S.** (2013). Principles and patterns of osmoregulation and euryhalinity in fishes. In *Fish Physiology*, Vol. 32 (ed. S. D. McCormick, A. P. Farrell and C. J. Brauner), pp. 1-44. San Diego, CA: Academic Press.
- Ern, R. and Esbaugh, A. J.** (2018). Effects of salinity and hypoxia-induced hyperventilation on oxygen consumption and cost of osmoregulation in the estuarine red drum (*Sciaenops ocellatus*). *Comp. Biochem. Physiol. A* **222**, 52-59. doi:10.1016/j.cbpa.2018.04.013
- Evans, D. H., Piemmarini, P. M. and Choe, K. P.** (2005). The multifunctional fish gill: dominant site of gas exchange, osmoregulation, acid-base regulation, and excretion of nitrogenous waste. *Physiol. Rev.* **85**, 97-177. doi:10.1152/physrev.00050.2003
- Ficke, A. D., Myrick, C. A. and Hansen, L. J.** (2007). Potential impacts of global climate change on freshwater fisheries. *Rev. Fish Biol. Fish.* **17**, 581-613. doi:10.1007/s11160-007-9059-5
- Fritz, E. S. and Garside, E. T.** (1974). Salinity preferences of *Fundulus heteroclitus* and *F. diaphanus* (Pisces: Cyprinodontidae): their role in geographic distribution. *Can. J. Zool.* **52**, 997-1003. doi:10.1139/z74-133
- Gibbons, T. C., McBryan, T. L. and Schulte, P. M.** (2018). Interactive effects of salinity and temperature acclimation on gill morphology and gene expression in threespine stickleback. *Comp. Biochem. Physiol. A* **221**, 55-62. doi:10.1016/j.cbpa.2018.03.013
- Gilmour, K. M. and Perry, S. F.** (2018). Conflict and compromise: using reversible remodeling to manage competing physiological demands at the fish gill. *Physiology* **33**, 412-422. doi:10.1152/physiol.00031.2018
- Gonzalez, R. J. and McDonald, D. G.** (1992). The relationship between oxygen consumption and ion loss in a freshwater fish. *J. Exp. Biol.* **163**, 317-332.
- Greaney, G. S. and Powers, D. A.** (1978). Allosteric modifiers of fish hemoglobins: *in vitro* and *in vivo* studies of the effect of ambient oxygen and pH on erythrocyte ATP concentrations. *J. Exp. Zool.* **203**, 339-349. doi:10.1002/jez.1402030302
- Greco, A. M., Fenwick, J. C. and Perry, S. F.** (1996). The effects of soft-water acclimation on gill structure in the rainbow trout *Oncorhynchus mykiss*. *Cell Tissue Res.* **285**, 75-82. doi:10.1007/s004410050622
- Griffith, R. W.** (1974). Environment and salinity tolerance in the genus *Fundulus*. *Copeia* **1974**, 319-331. doi:10.2307/1442526
- Hanrahan, J. W. and Tabcharani, J. A.** (1990). Inhibition of an outwardly rectifying anion channel by HEPES and related buffers. *Membr. Biol.* **116**, 65-77. doi:10.1007/BF01871673
- Henriksson, P., Mandic, M. and Richards, J. G.** (2008). The osmoregulatory compromise in sculpins: impaired gas exchange is associated with freshwater tolerance. *Physiol. Biochem. Zool.* **81**, 310-319. doi:10.1086/587092
- Hochachka, P. W. and Mommsen, T. P.** (1983). Protons and anaerobiosis. *Science* **219**, 1391-1397. doi:10.1126/science.6298937
- Hochachka, P. W., Buck, L. T., Doll, C. J. and Land, S. C.** (1996). Unifying theory of hypoxia tolerance: molecular/metabolic defense and rescue mechanisms for surviving oxygen lack. *Proc. Natl. Acad. Sci. USA* **93**, 9493-9498. doi:10.1073/pnas.93.18.9493
- Katoh, F. and Kaneko, T.** (2003). Short-term transformation and long-term replacement of branchial chloride cells in killifish transferred from seawater to freshwater, revealed by morphofunctional observations and a newly established "time-differential double fluorescent staining" technique. *J. Exp. Biol.* **206**, 4113-4123. doi:10.1242/jeb.00659
- Kidder, G. W., Petersen, C. W. and Preston, R. L.** (2006a). Energetics of osmoregulation: II. water flux and osmoregulatory work in the euryhaline fish, *Fundulus heteroclitus*. *J. Exp. Zool.* **305A**, 318-327. doi:10.1002/jez.a.252
- Kidder, G. W., Petersen, C. W. and Preston, R. L.** (2006b). Energetics of osmoregulation: I. oxygen consumption by *Fundulus heteroclitus*. *J. Exp. Zool.* **305A**, 309-317. doi:10.1002/jez.a.251
- Kirschner, L. B.** (1995). Energetics of osmoregulation in fresh water vertebrates. *J. Exp. Zool.* **271**, 243-252. doi:10.1002/jez.1402710402
- Kraemer, L. D. and Schulte, P. M.** (2004). Prior PCB exposure suppresses hypoxia-induced up-regulation of glycolytic enzymes in *Fundulus heteroclitus*. *Comp. Biochem. Physiol. C Toxicol. Pharmacol.* **139**, 23-29. doi:10.1016/j.cca.2004.08.015
- Laurent, P., Chevalier, C. and Wood, C. M.** (2006). Appearance of cuboidal cells in relation to salinity in gills of *Fundulus heteroclitus*, a species exhibiting branchial Na⁺ but not Cl⁻ uptake in freshwater. *Cell Tissue Res.* **325**, 481-492. doi:10.1007/s00441-006-0187-3
- LeBlanc, D. M., Wood, C. M., Fudge, D. S. and Wright, P. A.** (2010). A fish out of water: gill and skin remodeling promotes osmo- and ionoregulation in the mangrove killifish *Kryptolebias marmoratus*. *Physiol. Biochem. Zool.* **83**, 932-949. doi:10.1086/656307
- Lilly, L. E., Blinebry, S. K., Viscardi, C. M., Perez, L., Bonaventura, J. and McMahon, T. J.** (2013). Parallel assay of oxygen equilibria of hemoglobin. *Anal. Biochem.* **441**, 63-68. doi:10.1016/j.ab.2013.06.010
- Mallatt, J.** (1985). Fish gill changes induced by toxicants and other irritants: a statistical review. *Can. J. Fish. Aquat. Sci.* **42**, 630-648. doi:10.1139/f85-083
- Mandic, M., Todgham, A. E. and Richards, J. G.** (2009). Mechanisms and evolution of hypoxia tolerance in fish. *Proc. R. Soc. B Biol. Sci.* **276**, 735-744. doi:10.1098/rspb.2008.1235
- Mandic, M., Speers-roesch, B. and Richards, J. G.** (2012). Hypoxia tolerance in sculpins is associated with high anaerobic enzyme activity in brain but not in liver or muscle. *Physiol. Biochem. Zool.* **86**, 92-105. doi:10.1086/667938
- Marshall, D. J., Bode, M. and White, C. R.** (2013). Estimating physiological tolerances—a comparison of traditional approaches to nonlinear regression techniques. *J. Exp. Biol.* **216**, 2176-2182. doi:10.1242/jeb.085712
- Marshall, W. S., Tait, J. C. and Mercer, E. W.** (2016). Salinity preference in the estuarine teleost fish mummichog (*Fundulus heteroclitus*): halocline behaviour. *Physiol. Biochem. Zool.* **89**, 225-232. doi:10.1086/686037
- McBryan, T. L., Healy, T. M., Haakons, K. L. and Schulte, P. M.** (2016). Warm acclimation improves hypoxia tolerance in *Fundulus heteroclitus*. *J. Exp. Biol.* **219**, 474-484. doi:10.1242/jeb.133413
- McCormick, S. D., Moyes, C. D. and Ballantyne, J. S.** (1989). Influence of salinity on the energetics of gill and kidney of Atlantic salmon (*Salmo salar*). *Fish Physiol. Biochem.* **6**, 243-254. doi:10.1007/BF01875027
- Mitrovic, D. and Perry, S. F.** (2009). The effects of thermally induced gill remodeling on ionocyte distribution and branchial chloride fluxes in goldfish (*Carassius auratus*). *J. Exp. Biol.* **212**, 843-852. doi:10.1242/jeb.025999
- Morgan, J. D. and Iwama, G. K.** (1999). Energy cost of NaCl transport in isolated gills of cutthroat trout. *Am J Physiol Regul. Integr. Comp Physiol* **277**, R631-R639. doi:10.1152/ajpregu.1999.277.3.R631
- Mueller, C. A. and Seymour, R. S.** (2011). The regulation index: a new method for assessing the relationship between oxygen consumption and environmental oxygen. *Physiol. Biochem. Zool.* **84**, 522-532. doi:10.1086/661953
- Nikinmaa, M. and Huestis, W. H.** (1984). Adrenergic swelling of nucleated erythrocytes: cellular mechanisms in a bird, domestic goose, and two teleosts, striped bass and rainbow trout. *J. Exp. Biol.* **113**, 215-224.
- Nilsson, G. E.** (2007). Gill remodeling in fish—a new fashion or an ancient secret? *J. Exp. Biol.* **210**, 2403-2409. doi:10.1242/jeb.000281
- Nilsson, G., Löfman, C. O. and Block, M.** (1995). Extensive erythrocyte deformation in fish gills observed by *in vivo* microscopy: apparent adaptations for enhancing oxygen uptake. *J. Exp. Biol.* **198**, 1151-1156.
- Nilsson, G. E., Dymowska, A. and Stecyk, J. A. W.** (2012). New insights into the plasticity of gill structure. *Respir. Physiol. Neurobiol.* **184**, 214-222. doi:10.1016/j.resp.2012.07.012
- Perry, S. F.** (1998). Relationships between branchial chloride cells and gas transfer in freshwater fish. *Comp. Biochem. Physiol. A Mol. Integr. Physiol.* **119**, 9-16. doi:10.1016/S1095-6433(97)00411-X
- Perry, S. F.** (2011). Respiratory responses to hypoxia in fishes. In *Encyclopedia of Fish Physiology* (ed. A. P. Farrell), pp. 1751-1756. San Diego, CA: Elsevier Inc.
- Perry, S. F., Jonz, M. G. and Gilmour, K. M.** (2009). Oxygen sensing and the hypoxic ventilatory response. In *Fish Physiology* (ed. A. P. Farrell, C. J. Brauner and J. G. Richards), pp. 193-253. San Diego, CA: Academic Press.
- Pörtner, H. O. and Grieshaber, M. K.** (1993). Critical PO₂s in oxyconforming and oxyregulating animals: gas exchange, metabolic rate and the mode of energy production. In *The Vertebrate Gas Transport Cascade: Adaptations to Environment and Mode of Life* (ed. J. E. P. W. Bicuado), pp. 330-357. Boca Raton, FL: CRC Press.
- Potts, B. Y. W. T. W.** (1954). The energetics of osmotic regulation in brackish- and fresh-water animals. *J. Exp. Biol.* **31**, 618-630.
- Randall, D. J., Baumgarten, D. and Malysz, M.** (1972). The relationship between gas and ion transfer across the gills of fishes. *Comp. Biochem. Physiol. A* **41**, 629-637. doi:10.1016/0300-9629(72)90017-5
- Rao, G. M. M.** (1968). Oxygen consumption of rainbow trout (*Salmo gairdneri*) in relation to activity and salinity. *Can. J. Zool.* **46**, 781-786. doi:10.1139/z68-108
- Regan, M. D. and Richards, J. G.** (2017). Rates of hypoxia induction alter mechanisms of O₂ uptake and the critical O₂ tension of goldfish. *J. Exp. Biol.* **220**, 2536-2544. doi:10.1242/jeb.154948
- Richards, J. G., Sardella, B. A. and Schulte, P. M.** (2008). Regulation of pyruvate dehydrogenase in the common killifish, *Fundulus heteroclitus*, during hypoxia exposure. *Am. J. Physiol. Integr. Comp. Physiol.* **295**, R979-R990. doi:10.1152/ajpregu.00192.2008
- Rogers, N. J., Urbina, M. A., Reardon, E. E., McKenzie, D. J. and Wilson, R. W.** (2016). A new analysis of hypoxia tolerance in fishes using a database of critical oxygen level (P_{crit}). *Conserv. Physiol.* **4**, 1-19. doi:10.1093/conphys/cow012
- Sollid, J., De Angelis, P., Gundersen, K. and Nilsson, G. E.** (2003). Hypoxia induces adaptive and reversible gross morphological changes in crucian carp gills. *J. Exp. Biol.* **206**, 3667-3673. doi:10.1242/jeb.00594
- Sundin, L. and Nilsson, G. E.** (1998). Endothelin redistributes blood flow through the lamellae of rainbow trout gills. *J. Comp. Physiol. B* **168**, 619-623. doi:10.1007/s003600050184
- Taylor, M. H., Leach, G. J., Dimichele, L., Levitan, W. M. and Jacob, W. F.** (1979). Lunar spawning cycle in the mummichog, *Fundulus heteroclitus* (Pisces: Cyprinodontidae). *Copeia* **1979**, 291-297. doi:10.2307/1443417

- Thomas, S., Fievet, B., Claireaux, G. and Motais, R.** (1988). Adaptive respiratory response of trout to acute hypoxia. I. Effects of water ionic composition on blood acid-base status response and gill morphology. *Respir. Physiol.* **74**, 77-90. doi:10.1016/0034-5687(88)90142-9
- Urbina, M. A. and Glover, C. N.** (2015). Effect of salinity on osmoregulation, metabolism and nitrogen excretion in the amphidromous fish, inanga (*Galaxias maculatus*). *J. Exp. Mar. Bio. Ecol.* **473**, 7-15. doi:10.1016/j.jembe.2015.07.014
- Val, A. L.** (2000). Organic phosphates in the red blood cells of fish. *Comp. Biochem. Physiol. A* **125**, 417-435. doi:10.1016/S1095-6433(00)00184-7
- Völkel, S. and Berenbrink, M.** (2000). Sulphaemoglobin formation in fish: a comparison between the haemoglobin of the sulphide-sensitive rainbow trout (*Oncorhynchus mykiss*) and of the sulphide-tolerant common carp (*Cyprinus carpio*). *J. Exp. Biol.* **203**, 1047-1058. doi:10.21275/art20178943
- Wegner, N.** (2011). Gill respiratory morphometrics. In *Encyclopedia of Fish Physiology: From Genome to Environment* (ed. A. P. Farrell), pp. 803-811. San Diego, CA: Academic Press.
- Wells, R. M. G.** (2009). Blood-gas transport and hemoglobin function: adaptations for functional and environmental hypoxia. In *Fish Physiology*, Vol. 27 (ed. J. G. Richards, A. P. Farrell and C. J. Brauner), pp. 255-299. San Diego, CA: Academic Press.
- Wood, C. M.** (2018). The fallacy of the P_{crit} – are there more useful alternatives? *J. Exp. Biol.* **221**, jeb163717. doi:10.1242/jeb.163717
- Wood, C. M. and Grosell, M.** (2015). Electrical aspects of the osmorepiratory compromise: TEP responses to hypoxia in the euryhaline killifish (*Fundulus heteroclitus*) in freshwater and seawater. *J. Exp. Biol.* **218**, 2152-2155. doi:10.1242/jeb.122176
- Wood, C. M., Bucking, C. and Grosell, M.** (2010). Acid–base responses to feeding and intestinal Cl^- uptake in freshwater- and seawater-acclimated killifish, *Fundulus heteroclitus*, an agastric euryhaline teleost. *J. Exp. Biol.* **213**, 2681-2692. doi:10.1242/jeb.039164
- Zadunaisky, J. A.** (1984). The chloride cell: the active transport of chloride and the paracellular pathways. In *Fish Physiology* (ed. W. S. Hoar and D. J. Randall), pp. 129-176. Academic Press.